A REVIEW OF NUCLEAR ENERGY GENERATION IN STARS,

AND SOME ASPECTS OF NUCLEOSYNTHESIS

Hubert Reeves

Department of Physics
University of Montreal

and

Goddard Institute for Space Studies
National Aeronautics and Space Administration
New York, N.Y. 10027

(September 1964)

My aim will be threefold: 1) for each stage of stellar evolution, I will display the formula for the energy generation rate*; 2) I will discuss the uncertainties attached to each formula — uncertainties issuing both from the nuclear physics aspects of the problem and from possible variations in the chemical composition of the reacting material; 3) I will try to evaluate the size of the errors introduced in the analysis of stellar evolution when some minor nuclear reactions are neglected. (In other words, I shall try to find when these reactions can and cannot be neglected.) Because nuclear reactions produce new elements which may themselves become fuel at higher temperature, I shall consider some aspects of nucleosynthesis.

The basic equation describing the processes of energy generation and dissipation is

$$\frac{dL_r}{dM_r} = (\epsilon_N - \epsilon_\nu) + \frac{P}{\rho^2}\frac{d\rho}{dt} - \frac{du}{dt} \tag{1}$$

- 1 -

---

*Much of the material presented here is discussed in Reeves (1964) where references are given. Only new material is given in any detail.

This equation shows that the photon luminosity (per unit gram), dL_r/dM_r, can be created by nuclear energy processes ε_N, by doing work on the gas or by decreasing its internal energy u. The term ε_ν expresses the rate of energy dissipation by neutrinos. It may be worth mentioning that this formula implies the four basic interactions of modern physics: electromagnetic, nuclear, weak (neutrino emitting), and gravitational. In this talk I will consider only the nuclear and weak-interaction aspect of stellar energy generation.

In equation (1) I have grouped together the terms ε_N and ε_ν. This way $(\varepsilon_N - \varepsilon_\nu)$ becomes a kind of "effective" nuclear energy rate and can be treated as such along the lines of previous analysis of stellar interiors (e.g., Schwarzschild, 1957).

This term may become locally negative in a given star. During a nuclear burning stage this term must be mostly positive, or, more exactly

$$\int_M (\varepsilon_N - \varepsilon_\nu) \, dM_r > 0 , \tag{2}$$

as we cannot otherwise expect the gravitational energy term to vanish, hence the contraction to stop.

In cases where $(\varepsilon_N - \varepsilon_\nu)$ actually does become negative the luminosity will assume the following shape
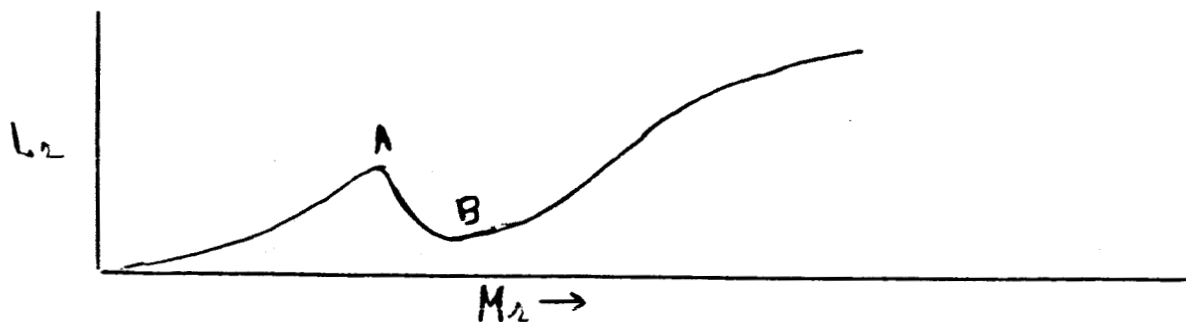
In the zone A → B photons are effectively being converted into neutrinos.

To determine the presence of such zones it is most useful to work with two parameters

$$n = d\ell n\ \epsilon\ /\ d\ell n\ T, \tag{3}$$

$$m = d\ell n\ \epsilon\ /\ d\ell n\ \rho\ . \tag{4}$$

n is called the temperature exponent and m the density exponent. Indeed we can write

$$\epsilon\ (T,\rho)\ =\ \epsilon_o\ (T_o,\rho_o)\ (T/T_o)^n (\rho/\rho_o)^m \tag{5}$$

where T_o and ρ_o are chosen in the range of interest for a given model. In this work I will quote the values of n and m for the various processes involved.

The behaviour of the late stages of stellar evolution is ultimately related with the possibility (or impossibility) of

- 3 -

creating neutrinos in process involving a direct coupling between electrons and neutrinos, e.g., in processes like $e^- + \gamma \rightarrow e^- + \bar{\nu}$ or $e^+ + e^- \rightarrow \nu + \bar{\nu}$. The physicists at CERN are now (1963) performing an experiment which may show the existence of the W^- particle: a charged vector boson expected to mediate the weak interactions. (I use the terms "may show" as some experts in the field have emphasized the difficulty of drawing any definite conclusions from such involved and complicated experiments.) The existence of the W^- would most likely imply the reality of these neutrino processes. As of today however the subject is still unsettled.

The presence (or the absence) of this extra mode of energy dissipation would alter considerably the time scales associated with the late stages of stellar evolution. Time scales may be evaluated (e.g., from star counts in various regions of the H.R. diagram). Hence observational results may eventually be used as critical tests for (or against) the reality of the neutrino processes under consideration.

In the present text, following the more or less general consensus of opinion, we shall assume the existence of these processes. Occasionally however we shall quote results which were computed without them, and discuss the difference.

Three types of neutrino producing mechanisms are expected to be important during the course of stellar evolution: plasma neutrinos, photoneutrinos and pair-annihilation neutrinos*. Their respective domains are mapped in Figure(1) together with the profile of iso-intensity. We shall discuss each of them in turn later.

The effect of these processes, together with the requirement stated in eqn. (2) seems to limit to four the maximum number of stellar nuclear-burning stages: hydrogen, helium, carbon, and oxygen burning. The time scale for neon photodisintegration is so short that the energy generated will at best slow down the contraction. (Nuclear reactions posterior to the fusion of oxygen will never be large enough to balance the tremendous output of neutrinos.

---

*Sakashita and Nishida (to be published) have called attention to another process: neutrino pair emission from excited nuclei. However its emission rate does in no condition appear to become as high as the sum of the rates of the three processes mentioned here.

Through the work of Hayashi (1962) and Salpeter (to be published) we have learned that all stars will not pass through the four stages. Stars with masses smaller than about the Chandrasekhar limit (when due corrections are applied) will give up somewhere along the path to become dwarfs. The limiting lower masses are about 0.1, 0.5 and 0.7 $M_\odot$ to qualify for Hydrogen, Helium and Carbon burning stages respectively.

HYDROGEN-BURNING-REACTIONS

Here we consider a number of reactions competent in burning four protons into one Helium[4] nucleus; yielding 6.68 MeV per nucleon (1 MeV/nucleon $\simeq 10^{18}$ erg/gm). The neutrino term ϵ_ν of eqn.(1) is, at best a few percent of ϵ_N, so that $(\epsilon_N - \epsilon_\nu)$ never becomes negative.

Proton-Proton Cycle

The energy generation rate is given by

$$\epsilon_{pp} = \epsilon (X_4 = 0) \Psi_{pp} (\alpha, W) . \qquad (6)$$

Here $\epsilon (X_4 = 0)$ is the rate of energy production if the core is devoid of Helium^4, $(X_4 = 0)$. (X_i will always be the fractional mass abundance of an isotope of mass number i). Ψ_{pp} then represent the effect of reactions induced by the He^4 nuclei themselves.

Numerically we have

$$\epsilon (X_4 = 0) = (2.06 \pm 0.2) \times 10^{16} f_{1,1} g_{1,1} \rho X_1^2$$
$$\exp (- 33.810 T_6^{-1/3}) T_6^{-2/3} \qquad (7)$$
$$T_6 = T \text{ in millions degrees } {}^{\circ}K.$$

The factor $f_{1,1}$ is the electron screening factor. For stars with $M > 0.6 M_{\odot}$ a very good approximation is $f_{1,1} = [1 + 0.25 \rho^{1/2}/T_6^{3/2}]$. For smaller stars more involved formalism must be used.

The factor $g_{1,1}$ is another correction term whose value is close to unity. It grows from the value 1.02 at $T_6 = 1$, to 1.09 at $T_6 = 15$, to 1.19 at $T_6 = 50$. The factor $\Psi_{pp} (\alpha, W)$ can be written down as

$$\Psi_{p,p}{}^{(\alpha, W)} = \{ 1 + \gamma [0.96 - 0.49 (W/1 + W)] \} \qquad (8)$$

We have $1 < \Psi_{p,p} < 2$; for $T_6 > 30$, $\Psi_{p,p} \simeq 1.46$.

The expression for γ is

$$\gamma = [(1 + 2/\alpha)^{1/2} - 1] \alpha \quad . \tag{9}$$

The value of γ grows from zero to one as the temperature increases. Then α, the term directly dependent on He^4 abundance, has the form

$$\alpha = 5.48 \times 10^{17} \ (X_4/4X_1)^2 \ \exp(- 100 \ T_6^{1/3}) \tag{10}$$

and finally,

$$W = 1.22 \times 10^{16} (1 + \rho^{1/2}/T_6^{3/2}) \ T_6^{-1/6} \ (1 + \frac{1}{X_1})^{-1}$$
$$\exp(- 102.6 \ T_6^{-1/3}) \quad . \tag{11}$$

The density exponent $m = 1$, and the temperature exponent are given with quite good accuracy by $n = (11.3/T_6^{1/3} - 2/3)$. At $T_6 = 15$, $n = 4$ while at $T_6 = 30$, $n \simeq 3$. In cases where the electron screening becomes important (small masses) the exponents can be altered to an appreciable extent and the above formula is no longer valid.

The governing reaction in the proton-proton cycle is the reaction $H' + H' \rightarrow D + e^+ + \nu$. This reaction can be thought of as going into two steps: a) formation of an excited

diproton; b) beta decay of the diproton into a deuteron. The main uncertainties come from the second part, as both the beta decay coupling constant and the matrix element for the transition are still slightly in doubt. The uncertainty or the rate is about 10%.

We must now consider a complex of minor reactions which are involved in the proton-proton cycle. First there is the $He^3 + He^3$. Our estimate is based from an experiment done at Oak Ridge in 1954. The people involved have assigned a 50% accuracy to their results. However the people at the California Institute of Technology have their doubts about that. They plan to redo the experiments. Fortunately because of the form in which this cross section comes in the formalism of the energy generation, even a large change would not alter the total rate to an appreciable extent. In the absence of a better estimate I will use the Oak Ridge value and uncertainty.

The rate of $He^3 + He^4$, through a recent experiment of Parker and Kavanagh (1963) is known to 15%. And the rate of the $Be^7 + p$ experiment is known to about 50%. These are the main uncertainties to worry about in the proton-proton cycle.

These effects on the total rate are rougly as follows: For $1 < T_6 < 10$ only the p + p reaction matters ($\simeq$ 10%). In the region from $10 < T_6 < 20$ and most sensitively around

$T_6 \simeq 14$ the reactions $He^3 + He^3$ and $He^3 + He^4$ bring in an extra source of uncertainty. The term α is known to about 60%. The term γ is relatively insensitive to α: in the worst case $\Delta\gamma/\gamma \simeq .20$ (at $\alpha \simeq 3$). In this region $W \ll 1$ so that $\Psi_{p,p} \simeq 1 + \gamma$ is known to better than 10%. Hence in the range $10 < T_6 < 20$ the rate is known to better than 15%.

In the next region $20 < T_6 < 30$, we have to consider the effect of the $Be^7 + p$ reaction. The expression W in eqn. (11) is known to about 50%. Its influence is most sensitively felt around $W \simeq 1$ ($T_6 \simeq 24$). It brings on Ψ_{pp} and uncertainty of about 4% (the effect of α is nil in that region). Here again the rate is known to better than 15%.

As you move toward higher temperatures Ψ_{pp} becomes constant, and only the $p + p$ uncertainty matters.

Errors in the evaluation of the chemical composition also influence our knowledge of the rates. The proton-proton reaction is proportional to X_1^2 (the hydrogen composition) but is also indirectly related to X_4 (the helium composition) through the term α in eqn. (9). If you change X_4 by a factor of two you never change Ψ_{pp} by more than 10%.

Carbon Nitrogen-Oxygen Cycle

Here the energy generation formula is

$$\epsilon_{CNO} = (7.9 \pm 0.8) \times 10^{27} \, f_{14,1} \, g_{14,1} \, \rho X_{14} X_1 \, T_6^{-2/3}$$

(12)

$$\exp(-152.31 \, T_6^{-1/3}) \quad \text{erg/gm/sec.}$$

with $f_{14,1} = [1 + 1.75 \, \rho^{1/2}/T_6^{3/2}]$, $g_{14,1} = [1 + 10^{-3}(3T_6^{1/3} - 4T_6^{2/3})]$, X_{14} is the fractional mass abundance of N_{14}.

The density exponent remains small (m = 1) while the temperature exponent ($n \simeq 50.8/T_6^{1/3} - 2/3$) becomes larger than ten in all cases of interest (for the sun $n \simeq 19.5$). For stars which draw most of their energy from this cycle such a high exponent drives the core into a convective state of energy transport. Such stars have central temperatures $T_6 > 18$. (For the sun $T_6 = 16$ and the energy contribution of this cycle is only 3%.)

At temperatures $T_6 > 16$ the cycle essentially transforms all the isotopes of carbon and nitrogen into N^{14}. Hence the term X_{14} in eqn. (12) is very closely equal to the initial abundance of these isotopes (Caughlan and Fowler, 1963). The same authors also show that at higher temperature the minor reactions $O^{16}(p,\gamma) \, F^{17}(e^+ \, \nu) \, O^{17}$, $O^{17}(p,\alpha) \, N^{14}$ will effectively throw in the game the O^{16} isotopes, thereby increasing correspondingly the value of X_{14}. Large uncertainties in the $O^{17}(p,\alpha) \, N^{14}$ rate make it difficult to evaluate with precision the onset of the transition.

As one approaches the very end of hydrogen-burning, a large number of minor reactions have to be taken into account. They have been considered by Parker et al (1964). Although their energetic contribution is usually very small, it may become crucial in short periods. Great care must be taken in handling these ends of stages.

After the exhaustion of hydrogen in the core, the nuclear burning of hydrogen takes place in a shell surrounding the core. The densities and temperature relevant to hydrogen burning both in the core and in the shell are pictured in Fig. (2) (from Hayashi's work). The periods spent in each region of the graph are marked on the curves. Such graphs serve as a basis to the study of nucleosynthesis of minor products in stars.

We note that in a star of medium mass (4 $M_\odot$), hydrogen burning in the core and in the shell takes place at very similar values of ρ and T. In bigger stars the shell burns at a quite larger temperature and slightly larger density.

Conditions in the contracting core are interesting for a study of the pre-helium-burning stage.

The nucleosynthetic effect of the hydrogen burning stage is the transformation of H, He, Li, Be, B into He^4 and the transformation of C N O F (and maybe Ne) in mostly N^{14} (~95%)

but also C^{12} (~4%) and C^{13} (~1%). In fact at the end of H-burning these ratios are not very much temperature dependent (Caughlan and Fowler 1963) and are characterized by the equalities

$$n_{12}P_{12,1} = n_{13}P_{13,1} = n_{14}P_{14,1} = n_{15}P_{15,1} \tag{13}$$

where $P_{12,1}$ is the probability of the reaction $C^{12}(p,\gamma)N^{13}$, and n_{12} is the number of C^{12} per unit volume. These equalities will be of importance to us later. In Pop II stars the fractional mass of N^{14} created this way is ~ 10^{-3}, while it is ~ 10^{-2} in Pop I stars.

HELIUM-BURNING-REACTIONS

C^{13} Substage. $C^{13}(\alpha,n)O^{16}$, Q = 2.215 MeV.

During the contraction phase the temperature becomes high enough for the reaction $C^{13}(\alpha,n)O^{16}$ to take place. The rate is approximately given by (Caughlan and Fowler, 1964)

$$\log (P_{13,4} / \rho X_4 f_{14,4}) = 17.1 - 2/3 \log T_8 - 30.2 T_8^{-1/3} \tag{14}$$

$$\log (\epsilon_{13,4} / X_{13}) = \log P_{13,4} + 17.2 \tag{15}$$

The rate is plotted in Fig. (3) (without electron screening, an important factor in small stars). The concentration of C^{13} varies from $X_{13} \simeq 10^{-5}$ (Pop II) to 10^{-4} (Pop I). The energy released in the entire fusion of C^{13} is 171 X_{13} KeV per nucleon in the gas. Even in a Pop. I star and even if the core material is highly degenerated (so that the nuclear energy release will heat the core instead of expanding it) the rise in temperature would be less than one million degrees. Consequently this reaction seems to have rather little influence on the course of stellar evolution.

Alan Liebman has used a sequence of models by Schwarzschild (1962) to investigate the onset and importance of this reaction (and of others to be described shortly) in a Pop.II star of 1.3 $M_{\odot}$ on its way to the helium burning phase. In Fig. (4) the energetic evolution of this star is described. L/M is the overall energy generation rate while L_{core}/M_{core} follows the contracting helium core itself (here most of the energy comes from hydrogen burning in a shell). In the model C^{13} (and N^{14}) burning are neglected. From the graph it is clear that even the largest reasonable amount of C^{13} ($X_{13} = 10^{-4}$) cannot play a significant role.

N^{14} Substage, $N^{14}(\alpha,\gamma)F^{18}$, Q = 4.404 MeV, $F^{18}(\beta^+,\nu)O^{18}$, Q = 1.677 MeV.

Later in the contraction phase N^{14} becomes combustible.
New data on this rate are analyzed in Appendix A3.   In the
range $0.4 < T_8 < 1.7$ the rate is given by

$$\log_{10} P_{14,4} / \rho X_4 f_{14,4} = -3.8 - 12.45 / T_8 - 3/2 \log T_8 \qquad (16)$$

$$\log \epsilon_{14,4} / X_{14} = 17.7 + \log P_{14,4} ,$$

$$n = 1 \quad n = [28.7/T_8 - 1.5]\,(\text{unscreened}) \qquad (17)$$

As this reaction will turn out to be important in small
stars (high densities and low temperatures) the electron
screening factor $(f_{14,4})$ will be large.   In many cases one will
meet the conditions of strong screening (Salpeter 1954).

The energy released by the fusion of N_{14} is 434 X_{14} keV
per nucleon in the gas.   In a Pop.I star ($X_{14} \simeq 10^{-2}$), with
degenerate core, this could correspond to a rise of several
tens of millions of degrees.   In Fig. (4) the effect is plotted
in the sequence of models of Dr. Schwarzschild (1962)(assuming
naively that this extra source of energy does not react on the
core).   Clearly this reaction could trigger the helium flash
(the lifting of degeneracy).   In smaller stars it could even
achieve the entire flash by itself.   The flash would best be

called the nitrogen-helium flash.

Hayashi has shown that stars with $M < 0.53\, M_\odot$ (Pop. II) or $M < 0.42\, M_\odot$ (Pop. I) cannot lift their temperatures high enough to allow the occurence of the $3He^4 \rightarrow C^{12}$ reaction, hence to qualify for the helium burning stage. The effect of the $N^{14}(He^4,\gamma)F^{18}$ reaction (neglected by Hayashi) should lower these limits, especially in the case of Pop. I stars. This will increase the differential mass range of white dwarfs of both populations.

Plasma Neutrinos

Around $T_8 = 1$ the emission of neutrinos by the plasma in stellar interior becomes important. Detailed calculations have been made by Inman and Ruderman (1964). The results are shown in Fig. (5).

One important parameter is the ratio (φ) of the plasma frequency ω_o to the thermal energy

$$\varphi = \hbar\, \omega_o / kT = \frac{3.34 \times 10^{-4}}{T_9} (\rho/\mu_e)^{1/2} \left[1 + 1.0 \times 10^{-4} (\rho/\mu_e)^{2/3} \right]^{-1/4} \qquad (18)$$

Here μ_e is the mean number of nucleon per electron ($\mu_e \simeq 2$). The line $\varphi = 1$ is plotted in Fig.(1). In the region $\varphi > 1$ the density and temperature exponents are given by

$$m \simeq 2.75 - \varphi/2, \quad n \simeq 1.5 + \varphi \qquad (19)$$

The temperature exponent is always much smaller than the exponents associated with nuclear reactions.

In Fig.(1) the plasma neutrinos are seen to be most intense around $\varphi \simeq 5.5$ (summit of the ridge). In Fig.(4) the energy dissipation L_ν by plasma neutrinos in the core of a 1.3 $M_\odot$ star during the pre-helium phase is plotted.

During most of the contraction phase L_ν is about ten times smaller than the gravitational energy generation of the contracting core, but it reaches about one third of this value at the end of the contraction, after the nitrogen flash. It seems that the nitrogen flash comes just in time to prevent this process from influencing appreciably the course of the evolution.

Helium Burning Stage. ($He^4 \rightarrow C^{12}$)

Around $T_8 = 1$ the reaction $3He^4 \rightarrow C^{12}$ becomes an important source of energy. The rate can be computed by methods of statistical mechanics or by ordinary reaction rate theory. The second way seems to give a rate twice as small as the first one, if one overlooks the fact that the Breit-Wigner cross section formula for identical particles (in allowed states) is twice as large as for non-identical particles (the geometrical factor is $2\pi\lambda^2$ instead of $\pi\lambda^2$). When this is taken

- 17 -

into account the results agree

$$(n_{12*} / n_4^3) = 3^{3/2} \lambda_\alpha^6 e^{-Q/kT} \qquad (20)$$

where n_{12*} is the number of excited C^{12} nuclei in a state at an energy
Q above the mass of $3He^4$, and $\lambda_\alpha = h/(2\pi M_\alpha kT)^{1/2}$.

The properties of the second excited level in C^{12} have been
reanalysed by the Brookhaven and the Cal. Tech. groups. The level is
an O^+ with $\Gamma_\gamma = 2.4 \pm 1.5$ meV, and $Q = 372 \pm 4$ keV . The reaction goes
resonantly through this level in the range $0.80 < T_8 < 6$.

The rate of creation of C^{12}

$$\log P_{3\alpha \to C^{12}} / (\rho X_4)^2 f_{3\alpha \to C} = -(6.72 \pm 0.25) - 18.9 \, T_8^{-1} - 3 \log T_8. \qquad (21)$$

and the rate of energy generation is

$$\log \epsilon_{3\alpha \to C} = \left[11.52 \pm 0.25 \right] + \log \left[f_{3\alpha \to C} \, \rho^2 X_4^3 \right] - 3 \log T_8 - 18.9 \, T_8^{-1} \qquad (22)$$

The uncertainty on the rate comes partly from Γ_γ and from Q.
The exponent m = 2 while n (unscreened) is given by:

n = 3 + 44.5/T_8, a very high value indeed.

The energy generation rate during helium burning also depends
on the subsequent reaction $C^{12}(\alpha, \gamma)O^{16}$. This is still a weak
point in our theory as its rate is poorly known. It can be written as

$$\log \left[P_{12.4} / \rho X_4 f_{12,4} \right] = 10.7 + \log (\theta_\alpha^2) - 30.05 \, T_8^{-1/3} - 2 \log T_8 \qquad (23)$$

The parameter θ_α^2 represents the fraction of the $C^{12} + He^4$ state in the 7.112 MeV level in O^{16}. Nothing is known about its value except that $\theta_\alpha^2 < 1$ and most likely > 0.01. It could in principle be determined by experiments but so far it has not been. Some authors have discussed its possible value in terms of alpha particle models ($\theta_\alpha^2 \simeq 1$) or collective models ($\theta_\alpha^2 \sim 0.78$ or possibly 0.024). At the present time it seems safer to use an intermediate value such as $\theta_\alpha^2 = 0.1$. The idea here is not to use an "average value" but to minimize the possible damage made on further theoretical development by an eventual experimental determination of this quantity.

On the $O^{16}(He^4, \gamma)Ne^{20}$ reaction ($Q = 4.730$ MeV), some very recent data is discussed in Appendix A 4. The rate becomes (in the range $2 < T_8 < 8$)

$$\log P_{16,4} / \rho X_4 f_{16,4} = (2.1 \pm 0.2) \times 10^2 \, T_8^{-3/2} \, 10^{-45.9/T_8} \qquad (24)$$

it is three time smaller than the rate given e.g. in (Reeves 1964). It is so much smaller than the rate of $C^{12} + He^4$ (for any reasonable value of θ_α^2) that except for very heavy stars $M \gtrsim 30 \, M_\odot$ the helium process never goes past the former reaction. Consequently we can write the total energy generation rate as:

$$e = e_{3He^4 \to C^{12}} \, \Psi_\alpha \qquad (25)$$

$$\Psi_\alpha = \left(1 + \frac{1}{3} \frac{Q_{12,4}}{Q_{3He^4 \to C^{12}}} \frac{X_{12}}{X_4^2} q_{16}\right) = \left(1 + 0.33 \frac{X_{12}}{X_4^2} q_{16}\right) \qquad (26)$$

$$\log{(q_{16}\rho)} = \left[\log\left(P_{12,4} \middle/ \rho \, X_4 \, f_{12,4} \right) - \log \left(P_{3\alpha - C^{12}} \middle/ \left(\rho \, X_4^2 \, f_{3\alpha - C^{12}} \right) \right) \right] \quad (27)$$

The term $P_{3\alpha \to C^{12}}$ is the rate of <u>formation of C^{12}</u> equ. (21).

Here $(q_{16}\rho)$ is independent of the density and of electron screening effects. It contains the term θ_α^2 and hence is very poorly known (about a factor of ten). This usually has rather little effects on the total energy generation rate since Ψ_α stays below two or three during most of the Helium burning phase. However Deinzer and Salpeter (1964) have shown that at the end of Helium burning $(X_\alpha < 0.1)$ Ψ_α will become very large, and there the uncertainty on θ_α^2 plays a major role.

To summarize: for stars with $M < 30 \, M_0$ the energy generation rate in Helium burning phase is given by eqs (25), (26), (27) and (22). The uncertainty in the rate is about a factor of two for $X_\alpha \gtrsim 0.3$. For $X_\alpha \lesssim 0.1$ the uncertainty could reach a value of order ten. This uncertainty may in turn deeply effect the determination of the trajectory of the star in the H. R. diagram

<u>Helium reactions in massive stars</u> $Ne^{20} (He^4, \gamma) Mg^{24}$
$Q = 9.314$ MeV); $Mg^{24} (He^4, \gamma) Si^{28}$, $(Q = 9.986$ MeV); $Si^{28} (He^4, \gamma) S^{32}$, $Q = 6.946$ MeV).

In stars with $M \gtrsim 30 \, M_\odot$ these reactions start contributing significantly to the energy generation rates.

Methods to evaluate these reactions and the uncertainties attached to them are described in Appendix A. We obtain

$$\log{(P_{20,4} / \rho \, X_4 \, f_{20,4})} = 19.7 - 43.75 \, T_8^{-1/3} - 0.09 \, T_8^{2/3} - 2/3 \log T_8 \quad (28)$$

$$\log{(P_{24,4} / \rho \, X_4 \, f_{24,4})} = 20.7 - 49.89 \, T_8^{-1/3} - 0.10 \, T_8^{2/3} - 2/3 \log T_8 \quad (29)$$

$$\log(P_{28,4} / \rho X_4 f_{28,4}) = 22.0 - \frac{2}{3} \log T_8 - 55.67 T_8^{-1/3} - 0.12 T_8^{2/3} \qquad (30)$$

In this case Ψ_α in equ. (26) becomes

$$\Psi_\alpha = 1 + \sum_{i=3} \frac{X_{4i} X_4^{-2}}{i} \frac{Q_{4(i+1)}}{Q_{3He^4 \to C^{12}}} q_{4(i+1)} \qquad (31)$$

where

$$\log \left[q_{4(i+1)} \rho \right] = \left[\log \left(P_{4i,4} / \rho X_4 f_{4i,4} \right) - \log \left(P_{3\alpha \to C^{12}} / (\rho X_4^2 f_{3\alpha \to C^{12}}) \right) \right] \qquad (32)$$

Here, clearly, i = 4 represents O^{16}, etc. With the proper Q values Ψ_α is given by

$$\Psi_\alpha = 1 + 0.328 X_4 X_{12} q_{16} + 0.162 X_4 X_{16} q_{20} + 0.256 X_4 X_{20} q_{24}$$

$$+ 0.229 X_4 X_{24} q_{28} + 0.136 X_4 X_{28} q_{32} .$$

Nucleosynthesis from Helium-Burning-Reactions

The regions of the ρ-T plane where Helium burning reactions are likely to be found (either in the core or in a shell during the carbon burning stage) are displayed Fig. (6) , again from Hayashi's work. (It should be remembered that neutrino emission has there been neglected. Its presence would affect the conditions of helium shell burning but not the conditions of helium core burning.)

To evaluate the nucleosynthetic effect of Helium the isotopic evolution has been followed till $X_\alpha \simeq 0.01$ assuming fixed temperature and density Fig. (7) . The curves are iso-abundance curves of various

elements. For instance the words $O^{16} > 50\%$ in a certain region mean that in the corresponding range of density and temperature the final product is mostly O^{16}. We noticed that Ne^{20} is almost by-passed; it appears only in a small region where it reaches at best a value of 10%. (By using extreme values for the rates a value of 20% could be obtained).

Salpeter and Deinzer (1964) and Hayashi (1962) have followed in detail, the isotopic evolution during Helium burning in the core for various masses. Salpeter and Deinzer start with initially homogeneous Helium stars, a simplification which may be of importance in assessing the accuracy of the predicted isotopic results. For the $O^{16}(He^4,\gamma)Ne^{20}$ rate they use successively $\theta_\alpha^2 = 0.1, 0.4, 1$. (Fig. (7) uses $\theta_\alpha^2 = 0.1$.) Their results are shown in Fig. (8). The final abundance of C^{12} and O^{16} depends very much on θ_α^2 but not the final abundance of heavier material. The isotopes Ne^{20} and Mg^{24} are essentially absent of stars with $M < 30M_\odot$. Even for larger masses Ne^{20} reaches at best 20% (these authors used older data which gave an $O^{16}(He^4,\gamma)Ne^{20}$ three times larger than the rate quoted here).

Hayashi's results on C^{12} and O^{16} in the Helium burning core are quite similar. He does not consider the generation of Ne^{20}. Hayashi's group has also studied the formation of C^{12} and O^{16} in a helium burning shell during carbon burning. For stars of 4 and 15.6 $M_\odot$ the temperature in the shell is very close to $T_8 = 2$, the density $\simeq 800$, the fractional carbon production is somewhat less than during helium core burning and the production of Ne^{20} (evaluated from their models) is at best a few percent.

The purpose of discussing these elements was to determine potential fuels for the following stages of evolution. It is of interest

however to attempt a comparison between these results and observational evidence on cosmic abundances. For such a comparison to be meaningful one would need a detailed theory of the restitution mechanisms of the evolved material to interstellar gas. Preliminary investigations have already been made on this matter. (Salpeter 1959)(Schmidt 1959). These authors make the assumption that stars with $M > 0.7M_\odot$ restitute an amount $\Delta M = (M-0.7M_\odot)$ to the interstellar gas at the end of their lives. Assuming further that the relative rate of star formation as a function of stellar mass has not changed since the beginning of the galaxy (the total rate has changed!) one finds that most of the gas came from stars with $2M_\odot < M < 5\ M_\odot$. (Stars with $M > 10\ M_\odot$ contribute virtually nothing.) The outer envelope, somehow expelled from such stars will contain, amongst other things, the product of helium burning reactions (mostly, presumably, from helium burning shells during later stages of evolution). The physical conditions in these shells still have to be computed, taking into account the neutrino emission processes. However from Figure (7) we can safely guess that the neon production will always be small.

Observationally, using the abundance of C, O, Mg in the sun (Goldberg, Mueller and Aller,1962) and the abundance of Ne^{20} from Suess-Urey "cosmic abundances" (Si^{28} is the standard) it

appears that of the group C,O,Ne,Mg,Si, about 20% belongs to carbon, 50% to oxygen, 20% to neon, and a few percent to magnesium and silicon. In view of the previous discussion the abundance of C and O are understandable but the abundance of Ne is very high. Since neon is also a product of carbon burning, most of it may come from there. Magnesium and silicon most likely come from the carbon burning stage, or from more advanced stages of stellar evolution.

Solar cosmic rays have recently been analysed by Biswas and Fichtel (1963). The analysis gives strong support to the view that, except for proton, the accelerating mechanisms do not disturb the original relative abundances. They find indeed the ratio of C/O in cosmic rays is very similar to the solar atmosphere C/O ratio. They have measured Ne^{20} (not spectroscopically detectable in the sun) and found it to be smaller than the above quoted value by a factor of about three. With their value one obtains: $X_C = 0.26$ $X_O = 0.58$ $X_{Ne} = 0.09$ $X_{Mg} = 0.04$ $S_{Si} = 0.04$.

The cosmic "normal" abundance of Ne^{20} has been evaluated from analyses of B stars, which according to Dr. Stromgren are very uncertain. The planetary nebulae typically have ratios of neon to oxygen which are about 10 times smaller than "normal" (Aller, private communication). It does not appear unreasonable

to argue that if there are any settings in our universe where we may hope to see the products of helium burning, unadulterated by nuclear processes associated with further stellar evolution, it is indeed in the gases which form the bulk of a planetary nebula.

Heavy elements build up in the helium burning phase.

The presence in nature of elements with $A > 56$ is attributed (BBFH 1957) to the turning on at a certain period (or periods) of stellar evolution of a rather large flux of neutrons. In particular, the existence of isotopes in the bottom of the valley of nuclear stability is proof of the action of neutron flux with characteristics such that the neutron capture time was much longer than beta decay lifetime of the unstable isotopes lining on both sides the bottom of the valley, and such that several tens of neutrons were absorbed per each seed nuclei (usually the metals, Co-Fe,Ni[*]). This process is called the s process, and the elements thus produced are called the s elements. In this respect the reaction $C^{13} (\alpha,n) O^{16}$ may be of importance since it generates neutrons, and hence may be a source of heavy element build-up. The C^{13} thus burned may have been left from H burning (as discussed before, the frac-
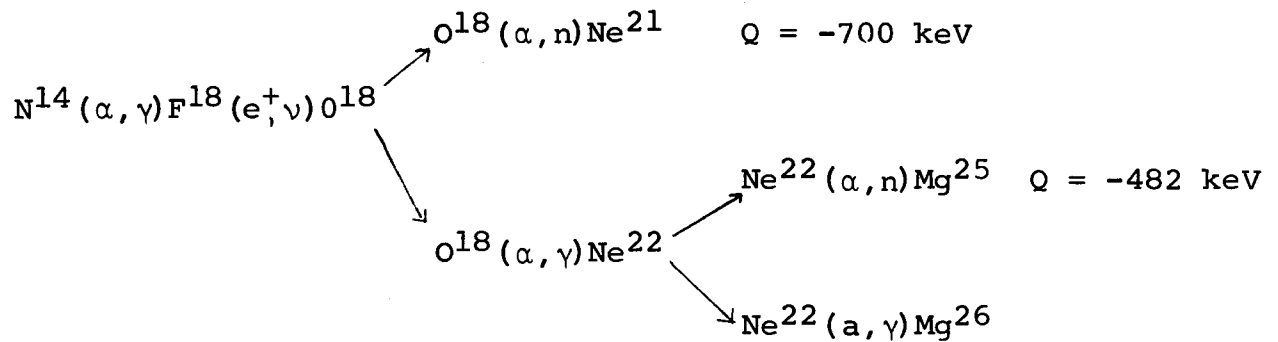
- 25 -

---

[*]For more details see Clayton et al(1961), Seeger,Fowler and Clayton(to be published).

tional mass of the CNO group to be found in the form of C^{13} is about 1%) or it may have been formed by mixing some protons to the helium burning core (Greenstein and Wallerstein, 1964). The effect of the originally present C^{13} is negligible for two reasons. First, even if every neutron were to be used for heavy element build-up, at best one neutron would be absorbed per metal nucleus. Second, there is the question of the N^{14} poison, about which however one must be careful. From Figure (3) it is evident that the atoms of C^{13} will always burn before the atoms of N^{14}, hence in the presence of these atoms. It is correct to say that through the $N^{14}(n,p) C^{14}$ reaction and its large cross section N^{14} will act as a neutron poison. But if the proton thus produced is then captured by a C^{12} atom, we shall have regeneration of the lost neutron by the reactions $C^{12}(p,\gamma) N^{13} \to C^{13}(He^4,n) O^{16}$. In other words C^{12} will act as an antidote to N^{14} poison, if it is abundant enough to capture a large fraction of the protons from the $N^{14}(n,p)$ reaction. Will that be our case? Clearly no, since in view of the hydrogen-burning-equilibrium-abundance ratio prevailing in the core (see eqn. 13), the proton has at best a 25% chance of being captured by a C^{12} neutron. Hence the formation of heavy elements from the original C^{13} is to be ruled out.

After the onset of helium burning the abundance of C^{12} will increase sharply and the situation would be reversed if C^{13} and N^{14} had managed to survive (which will never be the case) or if they had been produced by admixture of some hydrogen from the envelope. In this case C^{12} is a good antidote to N^{14} poisoning and heavy element build up is a possibility. Such mixing has been considered recently by Wallerstein and Greenstein (1964) in an attempt to explain the peculiar abundances found in CH stars.

In these stars carbon and the product of neutron capture process on a slow time scale (Ba, La, Ce, Nd) are enhanced considerably while oxygen is normal. The enhancement of C may imply that the neutron capture processes took place after the onset of the $3He^4 \rightarrow C^{12}$ reaction. The absence of O^{16} enhancement may imply that these processes took place rather shortly after the onset of the $3He^4 \rightarrow C^{12}$, and most likely at rather low temperature. As we shall discuss later, this gives strong support to the mixing mechanism advocated by Greenstein and Wallerstein.

Neutrons can also be generated by the sequence

$$O^{18}(\alpha,n)Ne^{21} \qquad Q = -700 \text{ keV}$$

$$N^{14}(\alpha,\gamma)F^{18}(e^+_,\nu)O^{18}$$

$$O^{18}(\alpha,\gamma)Ne^{22}$$

$$Ne^{22}(\alpha,n)Mg^{25} \quad Q = -482 \text{ keV}$$

$$Ne^{22}(a,\gamma)Mg^{26}$$

Because if its high threshold energy the branching

toward Ne^{21} is very difficult to achieve. It would occur if

N^{14} atoms were to be suddenly brought to temperatures $T_8 \simeq 4$

even for only a matter of seconds. Such conditions may be

met during the helium flash. In Schwarzschild's star (M = 1 3$M_\odot$)

T_8 = 3.4 is attained for a second or so. Evidently more detailed

models will be needed before we can evaluate the

importance of this mechanism in stars of smaller masses.

For heavier stars the lower branch is followed.

Two questions here: how far will the chain go before the

supply of He^4 is exhausted; if the chain is carried to the

end will the final products be $Mg^{26}+\gamma$ or $Mg^{25}+n$? To answer

these questions we must remember that at the end of helium

burning the main consumer of He^4 is C^{12}. From the graph it

appears that N^{14} and O^{18} will always burn before C^{12}, but not necessarily Ne^{22}. If the process takes place at $T_8 < 2$ Ne^{22} will be left intact; at higher temperature Ne^{22} burns and from the graph again we get mostly $Mg^{25} + n$, with a small fraction of Mg^{26}. With the abundances of N^{14} discussed before, this chain of reaction can yield as much as 100 neutrons per seed nuclei, probably enough to meet the requirement of the s process. At still higher temperature ($T_8 > 3$) Mg^{25} itself is reacting by $Mg^{25} (\alpha, n) Si^{28}$ to essentially double the output of neutrons. As a result we do expect sufficient neutron generation from N^{14} isotopes if the helium burning stage reaches a temperature of at least $T_8 = 2$ for a time sufficiently long to bring about a fairly complete exhaustion of Ne^{22} isotopes. Such temperatures are reached during the nitrogen-helium flash but for times which seem to be far too short (by factors of thousands, for instance in Schwarzschild's models). Studies of the flash for different masses may give a different answer but at present this seems to be extremely unlikely.

The proper combination of time and temperature are reached at the end of helium burning stages at least for rather massive stars (e.g., $M = 7M_\odot$ as studied by Hoffmeister et al, 1964). There however, we should expect the presence of s process elements such as Ba La Ce Nd to be accompanied by enhancement of C and of O.

To summarize: neutron will not be produced prior to the onset of helium burning. Small stars may get N^{14} generated neutrons during the helium flash; bigger stars do not get C^{13} or N^{14} generated neutrons in the early days of helium burning. Neutrons may appear through admixture of hydrogen, producing (if the enriched material eventually reaches the stellar surface) enhancement of carbon, and of s elements, but not necessarily of oxygen. Finally N^{14} generated neutrons will be produced at the very end of helium burning if the mass is large enough to bring the central temperature above $T_8 = 2$ before the He^4 is exhausted. From existing models, at least a few solar masses are needed for this to occur.

Photoneutrino Contraction Phase

This name is probably appropriate since in the contraction phase between helium burning and carbon burning this process becomes active and in fact, dissipates more energy than the photon emission processes. The switchover usually takes place in the range $T_8 = 3-5$.

The rate of energy generation is given by (Chiu, 1961)

$$\epsilon_\nu = 10^8\, T_9{}^8/\mu_e \quad \text{erg/gm/sec} \tag{33}$$

The term μ_e is the mean number of nucleons per electrons in the gas. Usually $\mu_e = 2$ (as for He^4, C^{12}, O^{16} etc.). However at higher temperature electron positron pairs will be produced, which must be taken into account in evaluating μ_e.

The density and temperature exponents are $m = 0$, $n = 8$. Again this is a rather small temperature exponent, as compared with the helium burning ($n \sim 30$) and the following carbon

burning (n $\simeq$ 30 also). This contraction phase will end when

the reaction $C^{12} + C^{12}$ will become fast enough to stop the

contraction. Shall we have a carbon flash? According to

Hayashi, Hoshi and Sugimoto (1962), no carbon flash will take

place if the photoneutrino process occurs. The core will

quietly warm up till the carbon burning reaction equals the

neutrino energy dissipation.

Carbon Burning Reactions

The Chalk River Group has recently studied very

thoroughly (experimentally and theoretically) the reactions

between C^{12} and a few light nuclei (C^{12}, N^{14}, O^{16}). The

elastic scattering data and the capture cross section data

have been improved to about 20% accuracy. Optical model

parameters have been obtained which match the data all through

the range of energy considered. In the Appendix A8 , a method is

described which allows a determination of the low energy part

of the capture cross section and hence a determination of the

thermonuclear reaction rate, most likely accurate to better

than a factor of three. The probability of a reaction is

given by

$$\log_{10} P/\rho X_C = (26.4 \pm 0.5) - \frac{36.55 (1 + 0.070 \ T_9)^{1/3}}{T_9} - 2/3 \ \log \ T_9 \qquad (34)$$

and the energy generation rate by

$$\log \epsilon_c = 17.7 + \log (P_{c+c} \ X_c) \ \text{erg/gm/sec} \qquad (35)$$

The range of temperature and density at which a star will stop its contraction to burn its carbon can be investigated by means of the following crude model. We assume first that the energy is almost entirely dissipated by neutrino emission. Several detailed models have shown this assumption to be valid. Then we find in the $\rho.T$ plane the locus of all the points representing conditions at the center of the star where carbon burning energy generation (assuming pure carbon) equals the neutrino energy dissipation. For temperature neighboring 10^9 we should include pair annihilation neutrinos (see Figure 1) which we shall discuss presently. This curve appears in Figure (10) under the label "first model". Correction has then been made to allow for the fact that neutrino emission takes place in a bigger volume than nuclear energy generation. This is the "corrected model" curve.

Hayashi has published models of stars in the carbon burning phase for which he neglects however the neutrino energy dissipation. He considers stars of $4M_\odot$ and $15.6M_\odot$, and sets at $0.7M_\odot$ the lower mass limit for a star to reach the carbon burning stage. In Figure (6) the evolution of the central density and temperature (together with the helium burning shells) are pictured. The H.R. diagram of the cluster h and χ Persei can be used to test the validity of the model.

There , two well defined types of giant stars appear; a group called early-type supergiants ($\simeq$ 22 stars) and a group called late type supergiants ($\simeq$ 15 stars). In between lies the Hertzsprung gap. Hayashi's evolutionary track after leaving the main sequence goes slowly through the first group, rapidly through the Hertzsprung gap and then slowly again through the second group. We expect the ratio of the period spent in each group to be similar to the ratio of the number of stars in each group. The ratio of the periods is about one in Hayashi's model (neglecting neutrino emission). Hayashi has calculated (although crudely) the reduction in the carbon stage period resulting from neutrino emission. He finds that the number of stars in the corresponding group should be down by a factor of about ten. Detailed models of carbon burning stars with neutrino emission would be desirable. If similar results are found, such evidence would work against the assumption of direct coupling between electrons and neutrinos (although the statistics here may not be really relevant).

Nucleosynthesis during carbon burning phase.

The reaction $C^{12} + C^{12}$ produces $Ne^{20} + He^4$ and $Na^{23} + H$ in roughly equal amounts. There is also a weak endothermic branching toward $Mg^{23} + n$ which we shall discuss later.

The abundance equations of carbon burning have been integrated for various carbon and oxygen initial abundances $(X_{12}{}^i + X_{16}{}^i = 1)$ for different sets of densities and temperature by Cameron (1959), Reeves and Salpeter (1959) and Tsuda (1963). The results are rather insensitive to the choice of ρ_c and T_c and to the (slightly different) choice of rate made by each author. They can be qualitatively described in the following way: (i denotes initial abundances and f denotes final abundances) (a) X_{16} remains the same $(X_{16}{}^i \simeq X_{16}{}^f)$; (b) $X_{20}{}^f$ is always less than $\simeq 0.35$; for $X_{12}{}^i < 0.40$, $X_{20}{}^i/X_{12}{}^i \gtrsim 0.6$, for $X_{12}{}^i > 0.40$: $X_{20}{}^f \simeq 0.30$; (c) $X_{24}{}^f/X_{12}{}^i \simeq 0.40$.

If the carbon reaction takes place at relative energy larger than 2.6 MeV the branching $Mg^{23}+n$ occurs about 5% of the time. (Bromley et al 1960) When the stellar central temperature is less than $T_9 = 0.8$ the neutron flux thus generated is negligible (see Appendix B).

On the other hand at $T_9 < 0.75$ substantial fluxes of neutrons become available through the following set of reactions initiated by the protons and He^4 emitted in the main branching: $C^{12}(p,\gamma)N^{13}(e^+,\nu)C^{13}(\alpha,n)O^{16}$. Calculations have shown that the $C^{12}(p,\gamma)N^{13}$ reactions occur mostly in the early days of the stage, and consequently in the lower temperature range of carbon burning. This way neutron fluxes capable of inducing about 50 neutron capture per metal nuclei could be released.

This source of neutrons is quenched at $T_8 > 7.5$ as then the isotope N^{13} photodisintegrates into $C^{12}+p$ before it has time to beta decay to C^{13}.

The introduction of pair annihilation neutrino processes has recently called for a reevaluation of the temperature at which the carbon burning stage will take place.

A combination of Hayashi's model (inhomogeneous models without neutrino emission) and Salpeter and Deinzer models (homogeneous models with neutrino emission) makes it clear that the carbon burning temperature ranges from $T_9 = 0.8$ to about 1.1. In the table the number of neutrons emitted per metal atom, assuming $X_{12} = 1/2$ $X_m = 5 \times 10^{-4}$ is given

T_8	0.6	0.7	0.8	0.85	0.9	1.0	1.1	1.2
No. of neutrons/metal	0.1	0.6	4	9	13	20	40	50

Clearly the $C^{12} + C^{12}$ burning stage provides an excellent source of neutrons and s element processing. Here the earmark would be probably the simultaneous enhancement of s elements and of Na^{23} (especially when compared to Mg^{24}). This statement cannot be proven simply. Qualitative analyses have shown it to be true in most cases of interest. In a naive way, however, one sees that each neutron absorbed leaves behind an Mg^{23} which

quickly decays to Na^{23} therefore increasing the concentration of this isotope. In real life one must still consider further reaction between all constituents of the gas. Na^{23} usually turns out to be still enhanced (as compared to the case where the branching ratio is shut) but not nearly as much . Detailed calculations would be needed to settle this matter.

From the previous paragraphs, s processing taking place during the carbon burning stage should also lead to enhancement of C^{12} (if the material is extracted before the end of the stage) O^{16}, Ne^{20} and Mg^{24} together with enhancement of s elements.

Pair-annihilation-neutrino contraction phase.

In the region $T_8 = 6$ the dominant emitting neutrino process passes from photoneutrinos to pair annihilation neutrinos (see Figs. (1) and (9)). For a nondegenerate nonrelativistic gas the energy generation rate is given by

$$\log \epsilon_{pair} = 18.7 - 5.15/T_9 + 3 \log T_9 - \log \rho \qquad (36)$$

with exponents $n = 11.9/T_9 + 3$, $m = -1$.

Neon-photodisintegration (flash?)

At $T_9 \simeq 1.25$ the contraction will be perturbed by the photodisintegration of $Neon^{20}$. The lifetime of an atom of Ne^{20} against photodisintegration is given by $\log_{10} \tau =$

$-(12.15 \pm 0.05) + 28.4/T_9$. Computation (Tsuda 1963) has shown that one half of the destroyed Neon becomes O^{16} and the other half becomes Mg^{24} (through $Ne^{20}(\alpha,\gamma) Mg^{24}$). The energy yield is about 2.3 MeV per initial neon atom. Hence

$$\log_{10} \epsilon = 29.2 - 28.4/T_9 \text{ erg/gm/sec.} \tag{37}$$

As discussed in the previous section the core at this coment contains about 25% Ne^{20} (in fractional mass). The photo-disintegration will yield $\simeq$ 600 KeV for each nucleus in the gas or $\simeq$ 30 KeV for each particle in the gas. In a partially degenerated core we may have a neon flash bringing us all the way up to the oxygen burning stage similar to the N^{14} flash. For large stellar masses the Ne^{20} photodisintegration will at best slow down the contraction towards the next stage.

At the end of this period, the isotopic abundance is roughly as follows: ($X_{12}^i + X_{16}^i = 1$ describes the results of the previous helium stage). (a) $X_{16} \simeq X_{16}^i + 0.15$; (b) $X_{20} \simeq 0$; (c) $X_{24} \simeq 0.4 X_{12}^i + 0.15$; (d) $X_{28} = 2$ to 4%.

Oxygen Burning Reactions

As the core temperature approaches $T_9 = 1.3 \simeq 1.4$ reaction between oxygen nuclei start releasing energy. Here experimental data is rather lacking. Only the $O^{16} (O^{16}, \alpha)Mg^{24}$ has been measured (Almqvist 1960) and the data extends only slightly

below the Coulomb barrier. More work is being done on that re-
action but is not available as of now   To an accuracy no better
than a factor of ten the following equation can be extracted from
the data

$$\log_{10} P / \rho X_O = 40.5 - 59.02 (1 + 0.14 \ T_9)^{1/3} - 2/3 \log T_9 \qquad (38)$$

with

$$\log \varepsilon_O = 17.8 + \log (P \ X_O) \ .$$

In Figure (12) the temperature and densities at which oxygen
and neon are expected to burn are described by using the crude
model described in the section on carbon burning. The nucleo-
synthetic effect of the oxygen burning stage has been studied
by Tsuda (1963) and Cameron (1959). The main outcome are the
elements from Mg^{24} to S^{32}. The elements Mg^{24}, Si^{28}, and S^{32}
are not really preponderant over in-between isotopes (as is the
case in cosmic abundances).

After the fusion of oxygen the emission of neutrinos becomes
so strong that nuclear energy generation most likely never
succeeds in halting the contraction. Hence we do not expect
any other burning stage. Nuclear reactions leading to the
equilibrium process have been considered by Hoyle and Fowler
(1964) and Tsuda and Tsuji (1963). They will not be discussed
here.

APPENDIX A

Thermonuclear reaction rates in the range $T_8 = 1$ to 50

For some (α, γ) (α, n) (p, γ) reactions, e.g., $Mg^{24}(\alpha, \gamma)Si^{28}$ the level scheme of the compound nucleus has been studied experimentally in a rather wide range of energy and the widths $\Gamma_\alpha, \Gamma_p, \Gamma_\gamma$ and the statistical factor $\omega = (2J+1)/(2I_t+1)(2I_i+1)$ have been determined for all the resonances E_r in that range. In such a case a lower limit to the rate can be obtained by adding the effects of each resonance

$$P/\rho\chi_1 = \sum_{\substack{\text{all} \\ \text{resonances}}} Pi/\rho\chi_1$$

$$\log Pi/\rho\chi_1 = 12.69 - 3/2 \log \mu - \log A_i + \log \left(\frac{\omega \, \Gamma_c \, \Gamma_n}{\Gamma}\right) \tag{A1}$$

$$- 3/2 \log T_8 - 50.4 E_r/T_8 \quad .$$

Here μ is the reduced mass, and Γ_c, Γ_n the widths for the charged particle and neutral particle reactions, respectively. This rate is a lower limit because of the contribution of resonances lying outside of the experimentally explored range. Because of experimental difficulties the (α, γ) reactions have not been brought below 1 MeV and the resonances in that range are expected to dominate the rate at $T_8 < 3$ or so. In Fig. (15) the position of the lowest measured resonances in Si^{28} are plotted against the background of the Gamow peak to illustrate the situation.

The total capture rate can also be evaluated by a combination of the information on individual resonances with data obtained from optical models of the nuclei. Here we take advantage of the experimentally discovered regularity of the optical model parameters, regularity best expressed in terms of the strength functions. In opposition to the case of neutron reactions, alpha reactions have so far failed to show structure in the individual partial wave (ℓ) strength functions. The sum of these strength functions appears to be energy independent, at least in ranges wide enough to be of use in the evaluation of thermonuclear reaction rates.

Through the optical model a computation of the capture cross section can be made. For alpha particle reactions, the nuclear potential is chosen to be of the form

$$V(r) = - (V_0 + iW_0)/ \{1 + \exp [(r-R_0)/_a]\} . \qquad (A2)$$

The best choice of parameters appears to be

$$V_0 = 50 \text{ MeV} \qquad W_0 = +10 \text{ MeV}$$

$$R_0 = (1.25 A_t^{1/3} + 1.6) f. \qquad a = 0.50 f.$$

(A_t is the mass number of the target nucleus.) (Vogt, private communication)

For proton reactions the real potential has the same form, with $V_0 = +55$ MeV, $R_0 = 1.25 A_t^{1/3}$, $a = 0.5f/$ The imaginary potential has a gaussian shape centered on the nuclear surface with

$\overset{.}{W}_g$ = +4 MeV. Calculations have been made by Chalk River workers on a Bendix G-20.

The results of these computations are then fitted by a formula of the form: (We use σ in barns, and E in MeV)

$$\sigma = \frac{S}{E}e^{-2\pi\eta}e^{-gE} = \frac{S}{E}e^{-0.98935(Z_1Z_2\mu^{1/2})/E^{1/2}}e^{-gE} \qquad (A3)$$

where g is left as a parameter determined in such a way as to make S energy independent up to the highest possible energy. Usually one can find a g such that S varies by less than 10% when the energy is varied from zero to about 60% of the Coulomb barrier energy $(B = Z_1Z_2e^2/R)$. Then S becomes a measure of the sum of the strength functions. If the computation had been made with the choice of a square well "black nucleus" the factor S would have taken the form (see Feshbach 1953)

$$S_{s,w} = \frac{2\pi^2\lambdabar^2}{E} \left[\xi_o^2 \sum(2\ell+1)G_o^2/G_\ell^2\right] \frac{1}{\pi KR} \qquad (A4)$$

The first factor can be written down as $2\pi^2\lambdabar^2/E = 4.126/\mu$, μ being the reduced mass. The term in the brackets represents the penetrabilities for all ℓ waves for a square nucleus of radius R. G_ℓ is the irregular Coulomb wave function. ξ_o^2, an almost energy independent parameter, is defined as

$$\xi_o^2 \equiv ye^{2\pi\eta}/\eta G_o^2 = 2y^{1/2}e^{4y^{1/2}}, \quad y = 2R_b/R; \quad R_b = [\hbar^2/\mu Z_1 Z_2 e^2].$$

The last term in eqn. (A3) is the value of the strength function for a black nucleus; $K \sim 1.4f.$ is the wave number inside the nucleus.

At energies much smaller than the Coulomb barrier and for $y^{1/2} > 4$ (as will be the case for our work on alpha capture reaction and $C^{12} + C^{12}$) the factor $\Sigma (2\ell+1) g_o^2 / g_\ell^2$ becomes independent of energy. Its value is plotted in Fig. (13).

Numerically the value of $S_{s,w}$ is closely given by

$$\log S_{s,w} = 0.1 + 1/2 \, \log\left(\frac{Z_1 Z_2}{\mu R}\right) + 0.458 [Z_1 Z_2 \mu R]^{1/2} \qquad (A5)$$

The results of optical model calculations for alpha capture by all the stable isotopes from C^{12} to S^{32} have been used to obtain the values of $S_{o,m}$ (optical model). All the values were very well represented by putting in the square well formula eqn. (A5) the choice $R_s = [1.50 \, A_1^{1/3} + 2.0]f.$ (Fig. 14)

In the square well formalism, the value of g is

$$g_{s,w} = y^{3/2}/6\eta^2 = 0.122 \left[\frac{\mu R^3}{Z_1 Z_2}\right]^{1/2} \, \text{MeV}^{-1} \qquad (A6)$$

with R in f, μ in a.m.u.

The values of g obtained from the optical model analysis have been plotted in Fig. (14) and tabulated in Table 1. It will be noted that they decrease somewhat rapidly with A_t the mass of the target. A sort of effective radius can be obtained by inverting the formula

$$R_g = 4.07 \left(\frac{Z_1 Z_2}{\mu}\right)^{1/3} g^{2/3} \, f \quad . \qquad (A7)$$

This time the radius R_g needed to reproduce g was of the form

$$R_g = 0.7 \, A_1^{1/3} + 4.0.$$

In a forthcoming paper (Vogt and Reeves, to be published) an analysis of the meaning of these parameters in terms of the structure of the nuclear well will be made.

Once S and g are found, the thermonuclear reaction rate becomes (S in MeV barns)

$$\log P/\rho x_1 = 10.56 + \log \left(\frac{z_1^{1/3} z_2^{1/3}}{A_1 \mu^{1/3}}\right) -2/3 \log T_8 + \log S$$

$$- 3.975 \left(\frac{z_1^2 z_2^2 \mu}{T_8}\right)^{1/3} (1 + 8.62 \times 10^{-3} g T_8)^{1/3} .$$

(A8)

In Table (1) the values of S, g and also the numerical constants necessary to compute the thermonuclear reaction rate are given (some of them have been slightly modified by the results of other techniques). To identify these constants we rewrite the eqn. (A8) in the form

$$\log P/\rho x_4 = M - 2/3 \log T_8 - N T_8^{-1/3} - PT_8^{2/3}$$

(A9)

Although the optical model usually gives a fairly good representation of the data, individual nuclei may at times depart from their expected behaviour. Then both S and g could influence the rate to any great extent.

As mentioned before, from the experimental determination of the individual resonances an evaluation of S can be made directly. If the resonances do not overlap to the point where

	log S(Mev b)	g(Mev^{-1})	M	N	P
C^{12} + He^4	6.45	.82	16.6	30.11	.07
C^{13} + "	6.55	.83	16.7	30.25	.07
N^{14} + "	7.22	.78	17.4	33.72	.08
N^{15} + "	7.29	.79	17.5	33.88	.08
O^{16} + "	7.95	.75	18.1	37.20	.08
O^{17} + "	8.04	.77	18.2	37.35	.08
O^{18} + "	8.14	.78	18.4	37.47	.08
F^{19} + "	8.73	.74	18.9	40.67	.09
Ne^{20} + "	9.44	.72	19.7	43.75	.09
Ne^{21} + "	9.39	.72	19.6	43.88	.09
Ne^{22} + "	9.47	.73	19.7	43.99	.09
Na^{23} + "	10.04	.70	20.3	46.97	.10
Mg^{24} + "	10.50	.68	20.7	49.89	.10
Mg^{25} + "	10.65	.69	20.9	49.97	.10
Mg^{26} + "	10.72	.69	21.0	50.06	.10
Al^{27} + "	11.25	.67	21.5	52.91	.10
Si^{28} + "	11.75	.66	22.0	55.67	.11
Si^{29} + "	11.82	.66	22.1	55.75	.11
Si^{30} + "	11.89	.67	22.1	55.82	.11
P^{31} + "	12.38	.66	22.7	58.56	.11
S^{32} + "	12.86	.63	23.1	61.16	.11

Table 1: Parameters for the computation of thermonuclear
reaction rates. (The temperature unit is $T_8 = 10^8 \, °K$)

interference phenomena become important, the cross section for

individual resonances can be written in the Breit Wigner fashion

$$\sigma = \pi \lambdabar^2 \, \omega \, \Gamma_c \, \Gamma_n \, / \, (E - E_r)^2 + \Gamma^2/4 \qquad \Gamma = \Gamma_c + \Gamma_n + \cdots \qquad (A10)$$

Averaging over resonances in an energy range ΔE

$$<\sigma> = \int \sigma dE \, / \, \Delta E = \Sigma \, 2\pi^2 \, \lambdabar^2 \, \Gamma_c \, \Gamma_n \, \omega \, / \Delta E \Gamma = \qquad (A11)$$

We define

$$\Gamma_{c,\ell} = \gamma_{c\ell} \, \xi_\ell^2 \, e^{-gE} \, e^{-2\pi\eta} \qquad = ye^{2\pi\eta}/\eta G_\ell^2 \qquad (A12)$$

where $\gamma_{c,\ell}$ is the reduced width and ξ_ℓ^2 an almost energy

independent factor representing angular momentum effects (ℓ).

If $\Gamma_c > \Gamma_n$ all through the range ΔE, we have

$$<\sigma> = \frac{S}{E} e^{-2\pi\eta - gE} \qquad (A13)$$

with

$$S = (2\pi^2 \lambdabar^2 \, E) \, \frac{\Sigma \, \omega \xi_\ell^2 \, \gamma_c}{\Delta E} = \qquad (A14)$$

$$2\pi^2 \lambdabar^2 E \Sigma_\ell \, \frac{<\omega \xi_\ell^2 \, \gamma_{c,\ell}>}{D_\ell} = [2\pi^2 \lambdabar^2 \, E] \, \xi_o^2 \, (\gamma_c/D) = \frac{4.126}{\mu} \, \xi_o^2 \, (\gamma_c/D) \; .$$

Here D_ℓ is the average distance between resonances of same (ℓ)

with orbital angular momentum (ℓ). The last term is a definition

of $\xi_o^2 (\gamma_c/D)$ based on the fact that the individual strength

function $< \gamma_c/D_\ell >$ are known to be practically energy

independent. Using the experimental values of $\Gamma_\alpha^{(exp)}$ we

calculate

$$\xi_o^2 (\gamma_c/D) = \sum_{\substack{\text{all} \\ \text{res. in } \Delta E}} \frac{\Gamma_\alpha^{(exp)} e^{2\pi\eta} e^{gE}}{\Delta E} \tag{A15}$$

On the other hand, when $\Gamma_c > \Gamma_n$

$$<\sigma> = 2\pi^2 \lambda^2 \sum_{\Delta E} \frac{\omega \Gamma_n}{\Delta E} = \frac{4.126}{\mu} \left\langle \frac{\Gamma_n}{D} \right\rangle \frac{1}{E} = \frac{C}{E} \tag{A16}$$

with C in MeV barns. The total rate involves the integral of

$<\sigma>v$ over all energies. However the range of energies where

$\Gamma_c < \Gamma_n$ bring a small contribution to the rate if the Gamow

energy E_o is above the energy (E*) for which $\Gamma_n = \Gamma_c$. Then we

write ($\mathcal{N}$ is Avogadro's number)

$$P/\rho\chi_1 = \frac{4\mathcal{N}}{A_1} \frac{1}{(2\pi\mu kT)^{1/2}} Ce^{-E^*/kT} \tag{A17}$$

or

$$\log P/\rho\chi_1 = 10.00 - \log A_1 - \frac{1}{2} \log \mu - 1/2 \log T_8 + \log C - 50.4E^*/T_8 \tag{A18}$$

The value of E* and C should really be obtained by trying to

fit the eqn.(A18) with the values obtained in eqn.(A1) by

- 46 -

summing over all resonances. If the measurements of individual

resonances are not available then we may use the value of S

obtained from the optical model calculation to get an average

value of $\dfrac{\Gamma_\alpha}{D}$ and by equating it to Γ_γ/D obtain E^*. That is

$$S = 2\pi^2 \chi^2 E \, \xi_0{}^2 \, (\gamma/D).$$

(A19)

$$\frac{\Gamma_\alpha}{D} = \xi_0{}^2 (\gamma/D) e^{-2\pi\eta} e^{-gE} = \omega \Gamma_{\gamma/D}) \text{ for } E = E^*$$

We discuss next the validity of the optical model approach

in the (low) temperature range where the widths of the Gamow peak

become comparable to the average spacing between resonances.

Except for a few nuclei, (p, γ), or (α, γ) reaction threshold are

to be found in energy regions of the compound nucleus where the

levels are fairly crowded. Typically the spacing of levels will

be of the order of 100 keV but larger distances between two

given levels will not be uncommonly found.

The use of optical models for thermonuclear reaction rates

clearly implies that at least a few resonances (or at least one

resonance with a more or less average reduced width) are to be

found inside the Gamow peak for any temperature under consideration.

Otherwise the method may overestimate the rate by several orders

of magnitudes.

The position and width of the Gamow peak are given by

$$E_O = 26.3(Z_1^2 Z_2^2 \mu)^{1/3} T_8'^{2/3} \text{ keV}$$

$$\Delta E_O = 35(Z_1^2 Z_2^2 \mu)^{1/6} T_8'^{5/6} \text{ keV} \tag{A20}$$

$$T_8' = [T_8/1 + 8.6 \times 10^{-3}g \, T_8], \quad g \text{ in MeV}^{-1}$$

Here ΔE_O is the full width at half maximum, g is defined in A3.

In the table the values of E_O and ΔE_O (in keV) are given

for typical protons and alpha reactions.

Z_1, Z_2	1,6	1,10	1,16	2,6	2,10	2,16
$\dfrac{\Delta E_O}{T_8^{2/3}}$	64	75	90	100	120	140
$\dfrac{E_O}{T_8^{5/6}}$	85	120	165	215	305	415

Clearly in the region $T_8 < 5$ important departure from the

assumption quoted in the previous paragraph may be expected.

If the corresponding level scheme is experimentally unknown

the determination of the rate becomes most uncertain. The rate

obtained from optical model calculations becomes essentially

an upper limit. A lower limit, an expected value and an estima-

tion of the uncertainty can be be obtained by throwing in more

nuclear statistics.

- 48 -

Experimentally the probability that two neighboring nuclear levels will be found at a distance D larger than a preassigned value D_O is well represented by the Wigner distribution formula

$$P\ (\ D > D_O) = \exp\ [-\Gamma/4\ (D_O/\overline{D})^2]\ \qquad (A21)$$

where $\overline{D}$ is the expectation value of D. The probability that two given resonances will be at $D > 3\overline{D}$ is about 0.001. For our purpose we restate this in the following way: our chances of finding one level at an energy E_r within $\Delta E = E_r - E_O = 1.5\ \overline{D}$ of the Gamow peak E_O is 99.9%. We define as our upper limit to the rate of the value obtained if the level is at the center of the peak (the rate is then closely equal to our optical model rate) and our lower limit, the value is obtained if the level is at a distance $E_r = E_O + 1.50\ \overline{D}$. The rate itself will be the geometrical means between these two values. The choice of 99.9% is arbitrary to an extent. It is however in the spirit of the determination of uncertainties by experimental physicists. Defining $u = \Delta E_O/E_O$, $v = (3.0\overline{D}/\Delta E_O)$ the ratio (f) of the lower limit to the upper limit is given by

$$f\ = P\ (E_r = E_O + 1.50\overline{D})\ /\ P(E_r = E_O)$$

$$= \exp\left[\ (-\tfrac{4}{3}u^2)\ (1 + uv + \frac{2}{(1+uv)1/2} -3)\ \right] \qquad (A22)$$

Consequently, we have $P_{max} = P$ (optical model) as in eqn. (9); $P_{min} = [P_{max} f]$ and we choose for the expected value and the uncertainty $[\log P \pm \Delta \log P] = [\log P \text{ (opt.mod.)} + 1/2 \log f] \pm 1/2 \log f]$.

The reduced widths themselves have a distribution given by

$$P(\gamma < \gamma_0) = \int_0^{x_0} e^{-x^2} \frac{2}{\sqrt{\pi}} dx \qquad x = \gamma/\overline{\gamma} \, , \tag{A23}$$

(so that $\gamma = \overline{\gamma} \pm 0.9\overline{\gamma}$ with a probability of $\simeq$ 90%). The correct way of doing this problem would be to analyze the probability function of the ratio (γ/D). However this is somewhat complicated for our purpose. With our previous choice of $D_0 = 3\overline{D}$ the chance of having two levels in the peak is itself 80% so that the fluctuation in the strength function averaged over the Gamow peak should probably not reach a value of more than three. A better estimate of $\log P$ should then be

$$\log P \pm \Delta \log P = \left[[\log P \text{(opt.mod.)} + 1/2 \log f] \pm (0.5 + 1/2 \log f) \right] \tag{A24}$$

In cases considered here, where the optical model has any interest $(O^{18}(\alpha, \gamma) Ne^{22}$, $Ne^{20}(\alpha, \gamma) Mg^{24}$, $Mg^{24}(\alpha, \gamma) Si^{28}$ etc.) the average level distance is about 100 KeV. Then 1/2 log f is about 0.8 at $T_8 = 1$, 0.3 at $T_8 = 2$, 0.15 at $T_8 = 3$ and 0.1 at $T_8 = 5$. Since we shall rarely need these reactions at temperature $T_8 < 3$, we have not considered this factor in the rate given in Table 1.

A-1 $C^{12}(\alpha,\gamma)O^{16}$ The rate is discussed in detail in Cartledge, Thibaudeau and Reeves (1963) and also in Reeves (1964).

A-2 $C^{13}(\alpha,n)O^{16}$ An estimate using an experimental measurement of the low energy non resonant contribution has been made by Caughlan and Fowler (1964). They obtain a value M = 17.1 while the optical model calculation yields 16.7.

A-3 $N^{14}(\alpha,\gamma)F^{18}$ The properties of the excited levels of F^{18} in the vicinity of 4,4 MeV can be inferred through an analysis of the $Ne^{20}(d,\alpha)$ and $O^{16}(He^3,p)$ reactions. (Enge and Wojtasek, 1959)

In particular, a level with T = 1 should be identified by the fact that the $\alpha + F^{18}$ outcome would be forbidden.

The relative intensity of alpha groups from the Ne^{20} + d reaction is given as

Energy of the level MeV	Relative Intensity
4.108	125
4.218	138
4.350	147
4.400	68
4.651	30
4.741	<7
4.844	70

Clearly the 4.741 level cannot participate in the reaction. It is most likely at T = 1 level. The 4.651 MeV level however is definitely active although its contribution is about four times smaller than the contributions of the other levels. Since the outcoming α have more than three MeV, the Coulomb effect is not important. The reduction probably reflects an unusually small value of θ_α^2, or a high angular momentum of the excited state, or both.

The reaction rate can be written as

$$\log P_{14,4}/\rho x_4 = 11.3 - 12.45/T_8 + \log \omega\Gamma_\alpha - 3/2 \log T_8$$

Following Brown (1962) we choose R = 5.6f for the radius of interaction. We obtain for $\omega\Gamma_\alpha$ of this level

$$\log \omega\Gamma_\alpha = -13.4 + \log (\omega\theta_\alpha^2) , \qquad (A25)$$

The average value of $(\omega\theta_\alpha^2)$ for levels of slightly higher energy is $\simeq 0.06$. Here, because of the low experimental yield we choose $\omega\theta_\alpha^2 = 0.02$ and obtain

$$\log P_{14,4}/\rho x_4 = -3.8 - \frac{12.45}{T_8} - \frac{3}{2} \log T_8 \qquad (A26)$$

This contribution to the total rate is dominant in the range

$0.4 < T_8 < 1.7$. At $T_8 > 1.7$, the contribution from the 4.844 MeV level becomes dominant. Using the same experimental data we obtain $\omega\theta_\alpha{}^2 = 0.05$ and

$$\log P_{14,4}/\rho x_4 = 2 - \frac{22.18}{T_8} - 3/2 \log T_8 \qquad (A27)$$

At temperatures $T_8 > 3$, the rate obtained from table ($\backslash$) should become valid.

A-4 $O^{16}(\alpha,\gamma)Ne^{20}$

Almqvist,E. and Kuehner,J.A., and also Evans et al (to be published 1964) report the following results from measurements of some properties of excited levels of Ne^{20}.

For the 5.63(3-) level

$\Gamma\gamma/\Gamma = 0.077 \pm 0.008$

$\Gamma = 1.9 \times 10^{-3}ev$, $(2\ell+1) \dfrac{\Gamma_\alpha \Gamma_\gamma}{\Gamma} = (1.0 \pm 0.1) \times 10^{-3}$ ev

For the 5.80 (1-) level

$$\Gamma\gamma/\Gamma < 3 \times 10^{-4}$$

The capture rate becomes

$$P_{16,4}/\rho x_4 = \frac{(2.1 \mp 0.2) \times 10^2}{T_8^{3/2}} \times 10^{-45.9/T_8} \qquad \text{(A28)}$$

in the range $2 < T_8 < 8$.

The photodisintregation rate

$$P_{16,4}^{dis.}/\rho x_4 = 10^{12.15} \times 10^{-28.4/T_9} \qquad \text{(A29)}$$

good

This last rate is within 10% at $T_8 < 8$ and is most likely

valid to $T_9 < 4$ (within 50%).

A-5 $O^{18}(\alpha,\gamma)Ne^{22}$ $O^{18}(\alpha,n)Ne^{21}$
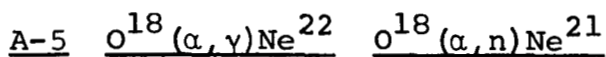
The rate can be computed from table (1). The neutron

branching ratio can be obtained by multiplying the rate of

$O^{18}(\alpha,\gamma)Ne^{22}$ by the ratio of neutron to total emission ratio as

discussed in Appendix B.

A-6 $Ne^{20}(\alpha, \gamma)Mg^{24}$

The experimental data covers the range $E_{c.m} = 2.073$ to 3.269 MeV, corresponding to $E^* = 11.387$ to 12.583 MeV in the Mg^{24} compound nucleus in which 11 resonances are reported. The value of $\xi_o^2(\gamma/D)$ was found to be $10^{9.47}$ and $S = 10^{9.56}$ as compared to $S = 10^{9.31}$ when calculated with the optical model.

A-7 $Mg^{24}(\alpha, \gamma)Si^{28}$

Here we have information in the range $E_{c.m} = 1.31$ MeV to 3.73 corresponding to $E^* = 11.296$ to 13.714 in the Si^{28} compound nucleus. We have $\xi_o^2(\gamma/D) = 10^{10.33}$ and $S = 10^{10.41}$. The optical model S is $10^{10.56}$. At temperature above $T_8 = 16$ (where $\Gamma_\gamma < \Gamma_\alpha$) we evaluate from the experimental data $(\Gamma_\gamma/D) = C = 1.4 \times 10^{-5}$. The best choice of E^*, both from the experimental data and from the calculation over the sum of the resonances is $E^* = 1.63$ MeV.

$$\text{This yield} \log P/\rho x_4 = 4.15 - 82.1/T_8 - 1/2 \log T_8 \qquad \text{(A30)}$$

In Figure 15 the rate computed by summing over the resonances is shown, together with the low temperature approximation (from Table (I)), and the high temperature approximation. As discussed before, the rate obtained by summing over the resonances is expected to underestimate the rate at both ends. In the graph the energy range where we have information on individual resonances

is shown with respect to the Gamow Peak. (Calculations by Jay Hauben)

A-8 $C^{12} + C^{12}$

The Chalk River group (Vogt,1964) has recently studied very thoroughly (experimentally and theoretically) the nuclear reactions between C^{12} and a few light nuclei (C^{12}, N^{14}, O^{16}). The elastic scattering and the capture cross section data have been improved to about 20% accuracy. The best fit to the data is obtained with the following set of parameters: $V_O = 50$ MeV, $W_O = 10$ MeV, $R_O = 5.77f$, $a \doteq 0.40f$. In Figure (16) the capture cross section thus obtained is compared with the experiments. Good agreement is obtained if the resonances are averaged over.

The lower range of the optical model calculation has been fitted by a formula of the form

$$\log \sigma = 17.30 - \log E - \frac{37.87}{E^{1/2}} - 0.35 E \tag{A31}$$

The resulting value of σ is plotted in Fig.(16). The difference between the optical model values and eqn.(A31) is less than 3% in the range 3.5 to 5.0 MeV. In the same range the cross section varies by a factor of more than four hundreds. The thermonuclear reaction rate can be written as

$$\log_{10} (P/\rho X_c) = 26.37 - \frac{36.55 (1+0.070 \, T_9)^{1/3}}{T_9^{1/3}} - 2/3 \log T_9 . \tag{A32}$$

In the range of stellar interest ($T_9 \simeq 0.7$) the formula (A32) gives a result which is about a factor of two smaller than the result given by Reeves (1962) or by Fowler and Hoyle (1964).

The uncertainty on the result has been brought down by quite a large amount. In view of the fact that the experimental results are good to 20% accuracy; that these results are well reproduced by the optical model; that the eqn.(A31)matches within a few percent the behavior of the optical model curve up to 0.60 of the Coulomb barrier energy, it is difficult to see how the rate eqn. (A32) could be wrong by more than a factor of three.

A-9 $Na^{23}(p,\alpha)Ne^{20}$ We have detailed information for incident proton energy (center of mass) varying from 100 keV to 778 keV.

The thermonuclear reaction rate has been computed by summing over the resonances and also by using the average reduced value of $\omega\Gamma_\alpha\Gamma_p/\Gamma$ as calculated from the first 14 resonances. Using the method described in Appendix A we get

$$\sum_{res} \frac{\omega\Gamma_\alpha\Gamma_p}{\Gamma} \; e^{2\pi\xi} \; e^{gE} = 10^{2.60} \tag{A33}$$

The Coulomb factor used in eqn.(A33) is the proton factor. We neglect the alpha Coulomb factor since the Q value for $Na^{23}(p,\alpha)Ne^{20}$ is already 2.3 MeV. This approximation should be reasonably good. The rate is then given by the formula

$$\log P_{23.1}/\rho X_1 = 14.15 - 19.43\ T_8^{-1/3} - 2/3\ \log\ T_8 - 0.02\ T_8^{2/3} \qquad (A34)$$

In the Figure 17 the lower curve represents the sum over individual resonances for the $Na^{23}(p,\alpha)\ Mg^{24}$ while the upper curve is computed from the formula. The sum over resonances represents accurately the thermonuclear reaction rate in the range $T_8 < 10$. Above this temperature high resonances (for which we have no information) start to contribute. Then the upper curve should be better. As we expect $\Gamma_p \simeq \Gamma_\alpha$ in this range, this curve probably overestimates the rate by a factor of two or so.

APPENDIX B

Production of neutrons through endothermic branching of
thermonuclear reactions between charged particles.

A. Fractional number of reactions taking place with
relative energies higher than a threshold energy E_t.

$$F = \int_{E_t}^{\infty} \sigma(E) n(E) v dE \Big/ \int_{0}^{\infty} n(E) \sigma(E) v dE$$

$$= \left[\int_{E_t}^{\infty} \exp[-E/kT' - a/E^{1/2}] dE \right] \Big/ [e^{-\tau} \Delta E_o \sqrt{\pi}/2]$$

(B-1)

where $a/E^{1/2} = 2\pi\eta$, $\tau = 3E_o/kT'$, $E_o^{3/2} = akT'/2$, $\Delta E_o = 4E_o/\sqrt{\tau}$,
T' has been defined in Appendix A. Here the integral in the
denominator has been evaluated with the usual method of re-
placing the integrand by a properly adjusted Gaussian. The
treatment of the numerator requires a little more attention.
We now define $E/E_o = x$, $E_t/E_o = x_t = 1 + u_t$ (we consider only
$u_t > o$), and $y = x_t - x$. Then we develop the integrand in the
numerator of eqn. (1) in a series in power of y (including
terms up to y^2)

$$E/kT' + a/E^{1/2} = x_t + \frac{2}{x_t^{1/2}} + y\left[1 - \frac{1}{x_t^{3/2}}\right] + y^2 \frac{3}{4} \frac{1}{x_t^{5/2}} + \ldots \quad \text{(B-2)}$$

Now inserting this development in eqn.(1) and integrating

we get,

$$F = \frac{x_t^{5/4}}{2} [1 - \varphi(z_t)] \exp \left[\frac{\tau}{9} (x_t^{5/2} - 5x_t - \frac{5}{\sqrt{x_t}} + 9) \right] \qquad (B-3)$$

where

$$z_t = \sqrt{\tau/3} (x_t^{5/4} - x_t^{-1/4})$$

and

$$\varphi(z_t) = \int_0^{z_t} (2/\sqrt{\pi}) \exp (-z^2) dz$$

as tabulated e.g., in Jamke-Emde, page 24.

Useful approximations:

for $u_t \ll 1$, $(x_t^{5/2} - 5x_t - \frac{5}{\sqrt{x_t}} + 9) \simeq (15/8 \ u_t^3 - 45/32 \ u_t^4)$ and

$$F \simeq [1 - \varphi(z_t)] \ ;$$

for $u_t \geqslant 0.5$, $F \simeq \frac{kT}{\Delta E_o} \frac{\exp\left[-\frac{\tau}{3}(x_t + 2/\sqrt{x_t} - 3) \right]}{(1 - x_t^{-3/2})}$. $\qquad (B-4)$

B. Average number of neutrons emitted per collision.

Here we need

$$g = \int_{E_t}^{\infty} \sigma(E) n(E) v dE (\Gamma_n/\Gamma) \bigg/ \int_0^{\infty} \sigma(E) n(E) v dE \qquad (B-5)$$

where Γ_n/Γ is the ratio of the neutron width to the total width

of the levels of compound nucleus, and E_t, here, becomes the threshold energy for neutron emission. The ratio (Γ_n/Γ) is small only for $(E-E_t)$ less than a few keV. In the rest of the energy range its value remains roughly constant. Depending upon the reaction under consideration it takes values ranging from (Γ_n/Γ) 1 to $\simeq 0.1$. Neglecting the lowest part of the range the average number of neutrons emitted per collision becomes

$$g \simeq (\overline{\Gamma_n/\Gamma}) \; F$$

$\underline{O^{18}(\alpha,n)Ne^{21}}$ $Q = -700$ keV. In the range of interest $(\Gamma_n/\Gamma) \simeq 1$ since Γ_α is still fairly small because of Coulomb effects and no other channel is open $(Q(\alpha,p) \simeq -5.7$ MeV). As a function of temperature we obtain

T_8	x_t	z_t	F	g
2.0	1.78	3.27	$\simeq 10^{-3}$	$\simeq 10^{-3}$
3.0	1.36	1.38	0.05	0.05
3.5	1.22	0.85	0.17	0.17
4.0	1.12	0.44	0.31	0.31

Here g is also the number of neutrons produced per each O^{18} nucleus in the gas. We notice that at higher temperature this number will be doubled by the $Ne^{21}(\alpha,n)Mg^{24}$ reaction.

$$\underline{Ne^{22}(\alpha,n)Mg^{25}} \qquad\qquad Q = -482 \text{ keV}$$

For the same reasons as in the previous case we expect $(\overline{\Gamma_n/\Gamma}) \simeq 1$ as we have $Q(\alpha,p) = -3.5$ MeV.

T_8	x_t	z_t	F	g
1.5	1.26	1.23	0.07	0.07
2.0	1.04	0.20	0.38	0.38

Again g is the number of neutrons per Ne^{22} nuclei. Higher temperature may double the crop of neutrons if enough He^4 are still present by then.

$$\underline{C^{12}(C^{12},n)Mg^{23}} \qquad\qquad Q = -2.603 \text{ MeV}.$$

The experimental evidence (Bromley 1960) gives a branching ratio of 0.05 (fairly constant) from 10 MeV down to 5 MeV in the center of mass system.

In the lower energy range two channels are still widely open $\left[(C^{12},\alpha); Q = 4.619 \text{ MeV}, (C^{12},p); Q = 2.230 \text{ MeV} \right]$. It is probably reasonable to assume that the value $(\overline{\Gamma_n/\Gamma}) = 0.05$ is valid at lower energies, although this may be uncertain by a factor of two or three.

To evaluate F we use $E_o = 2.418 (T'_9)^{2/3}$, where $T'_9 = T_9/(1 + 0.070\, T_9)$, as discussed in Appendix A.

T_9	x_t	z_t	F_{app}	$g/2$	F_{exact}
0.6	1.56	2.82	5.9×10^{-4}	2×10^{-5}	5.5×10^{-4}
0.7	1.41	2.02	8.8×10^{-3}	1.5×10^{-4}	7.1×10^{-3}
0.8	1.30	1.41	0.045	1×10^{-3}	0.036
0.85	1.25	1.18	0.079	2×10^{-3}	0.065
0.9	1.20	0.97	0.12	3×10^{-3}	0.105
1.00	1.13	0.58	0.24	0.005	0.215
1.10	1.06	0.28	0.37	0.01	0.373
1.20				0.012	0.487

As each collision takes two C^{12}, we have listed in the last
column $g/2$, the number of neutrons per C^{12} in the gas. In the
last column the exact value of F (computer integrated) is given
(calculations by E. Milford).

Just as an illustration we may consider five red giant stars which show very different composition. In the table the ratio of iron to hydrogen $(N_{Fe}/N_4$, related to the activity of the e process); the ratios of Ba-La-Ce-Nd to Fe, $(N/N_{Fe}$, related to the activity of the s process) and the ratios of C and O to Fe, (possibly related to the moment of occurrence of the s process) are given. The solar abundances are used as a standard.

Star	(N_{Fe}/N_H)	(N_s/N_{Fe})	(N_C/N_{Fe})	(N_O/N_{Fe})
Sun	1	1	1	1
HD122563	$\simeq$ 0.01	0.02		
HD165195	$\simeq$ 0.01	$\simeq$ 1		
HD201626	0.03	15	5	< 1.6
HD26	0.2	15	5	< 0.5
ϵ Virginis	1	1	1	1

References: Wallerstein (1964), Wallerstein et al (1963).

The question of whether evolved material can be brought to the surface of a star during its quiet lifetime is by no means settled. In this discussion we shall naively assume that such transport takes place at least in red giants. This assumption

is not very important. A similar discussion could be made on the content of the interstellar gas from which these stars were made if the transport assumption is wrong (or crude).

The ratio of N_{Fe}/N_H is thought to be related to the age of the star. The two first stars (apparently very old) are quite similar in many abundances (not quoted here) except for their s process abundance. This may reflect the fact that as shown above, neutron processes are not an automatic consequence of helium stage (and of more advanced stages) but depend amongst other things upon the stellar masses. The two following stars present evidence of intense neutron activity (increase in the s process elements). The enhancement of C without enhancement O suggests that the process took place in the early days of helium burning, possibly from proton admixture or from N^{14} burning at high temperature in the peak of the helium flash.

Finally ε Virginis is given as an example of "normal" red giants, in many ways similar to the sun.

Let it be emphasized that these analyses (and others in the text) are very preliminary and serve mostly as illustrations.

APPENDIX D

Table of Q Values for Various Reactions

Target   Q Values   MeV

	(p,γ)	(p,α)	(p,n)	(α,γ)	(α,n)
C^{12}	1.943	−7.557	−18.390	7.161	−8.507
C^{13}	7.549	−4.064	−3.004	6.357	2.214
N^{14}	7.291	−2.922	−5.931	4.404	−4.737
N^{15}	12.125	4.964	−3.543	4.012	−6.430
O^{16}	0.598	−5.218	−−	4.730	−12.145
O^{17}	5.597	1.193	−3.544	7.347	0.588
O^{18}	7.992	3.980	−2.450	9.667	−0.700
F^{19}	12.844	8.114	−4.031	10.465	−1.949
Ne^{20}	2.454	−4.132	−16.100	9.314	−7.221
Ne^{21}	6.743	−1.750	−4.305	9.885	2.555
Ne^{22}	8.790	−1.675	−3.624	10.616	−0.482
Na^{23}	11.693	2.379	−4.842	10.098	−2.971
Mg^{24}	2.287	−6.859	−14.800	9.986	−7.193
Mg^{25}	6.301	−3.142	−5.044	11.133	2.655
Mg^{26}	8.272	−1.826	−4.797	10.650	0.036
Al^{26}	7.471	−1.871	−−	10.417	−0.910
Al^{27}	11.581	1.594	−5.598	9.664	−2.652
Si^{28}	2.735	−7.700	−14.580	6.946	−8.135
Si^{29}	5.585	−4.832	−5.743	7.111	−1.532
Si^{30}	7.286	−2.378	−5.030	7.917	−3.504
P^{31}	8.863	1.917	−6.218	6.998	−5.572
S^{32}	2.285	−4.211	−13.780	6.641	−8.628
S^{33}	5.218	−1.526	−6.358	6.792	−2.002
S^{34}	6.367	−0.631	−6.203	7.213	−4.629
Cl^{35}	8.506	1.865	−6.763	7.213	−5.866
S^{36}	8.402	0.544	−1.920	6.809	−3.066
A^{36}	1.890	−4.355	−−	7.044	−8.685

REFERENCES

E. Almqvist and J.A. Kuehner, (To be published 1964).

S. Biswas and C.E. Fichtel, Ap. J. 139, 941 (1964).

D. A. Bromley, J.A. Kuehner and E. Almq ist, Phys. Rev. Letters . 4, 365 (1960).

R. E. Brown, Phys. Rev. 125, 347 (1962).

E.M. Burbidge, G.R. Burbidge, W.A. Fowler and F. Hoyle, , Rev. Mod. Phys. 29, 547 (1957).

A. G. W. Cameron, Ap. J. 130 , 916 (1959).

A. G. W. Cameron, Ap. J. 130, 452 (1959).

A. G. W. Cameron, Nuclear Astrophysics (To be published).

W. Cartledge, M. Thibaudeau and H. Reeves, Publications of the Institute for Space Studies (New York City, 1963).

G. R. Caughlan and W.A. Fowler, Ap. J. 136, 453 (1963).

G. R. Caughlan and W. A. Fowler, Ap. J. 139, 1180 (1964).

H. Y. Chiu, Phys. Rev. 123, 1040 (1961).

D.D. Clayton, W.A. Fowler, T. E. Hull, and B.A. Zimmerman, Ann. Phys. 12, 331 (1961).

W. Deinzer and E.E. Salpeter (To be published 1964).

H. Enge and J. H.Wojtasek, M.I.T. L.N.S. Progr. Rep. (Nov.,1959).

E. Evans et. al (To be published 1964).

H. Feshback, M.M. Shapiro and V. F. Weisskopf, Tables of Penetrabilities of Charged Particle Reactions, N.Y.O.-3077 (1953).

L. Goldberg, E. A. Müller and L.H. Aller, Ap. J. Suppl. 5, 1-138 (1960).

J. L. Greenstein and G. Wallerstein, Ap. J. 139 , 1163 (1964).

C. Hayashi, R. Hoshi and D. Sugimoto, Prog. Theor. Phys. Suppl. 22 (1962).

E. Hoffmeister, R. Kippenhohn and A. Weigert, Zeitschrift für Astrophysik 59, 215 (1964).

F. Hoyle and W.A. Fowler, Ap. J. Suppl. 91 (1964).

C. L. Inman and M.A. Ruderman, Publications of the Institute for Space Studies (1964).

P.D. Parker, J. N. Bahcall and W.A. Fowler, Ap. J. 139, 602 (1964).

P.D. Parker and R.W. Kavanagh, Phys. Rev. 131, 2578 (1963).
H. Reeves, To be published in Vol. 8, Stars and Stellar Systems (1964).
H. Reeves and E. E. Salpeter, Phys. Rev. 116, 1505 (1959).

S. Sakashita and M. Nishida, Prog. Theor. Phys. 31, 227 (1964).

E.E. Salpeter, Ap. J. 129, 608 (1959).

E.E. Salpeter, Austral. J. Phys. 7, 373 (1954).

M. Schmidt, Ap. J. 129, 243 (1959).

M. Schwarzschild, Structure and Evolution of Stars (Princeton University Press, Princeton, 1958).

M. Schwarzschild and H. Selberg, Ap. J. 136, 150 (1962).

P.A. Seeger, W.A. Fowler and D.D. Clayton (To be published).

H. Tsuda and H. Tsuji, Prog. Theor. Phys. 30, 34 (1963).

H. Tsuda, Prog. Theor. Phys. 29, 29 (1963).

E. W. Vogt, D. McPherson, J. Kuehner and E. Almqvist (To be published 1964).

G. Wallerstein, J. L. Greenstein, P. Parker, H. L. Helfer and L. H. Aller, Ap. J. 137, 280 (1963).

Figure 1. Iso-intensity curves for emission of neutrinos in
the ρ-T plane. The label on each curve identifies the
energy yield in erg/gm/sec along that line. Three processes
are considered: plasma neutrinos, photoneutrinos, pair
annihilation neutrinos. The dashed parts of the curves
reflect the fact that photoneutrino rates in degenerate
matter have not yet been properly computed.

Figure 1.
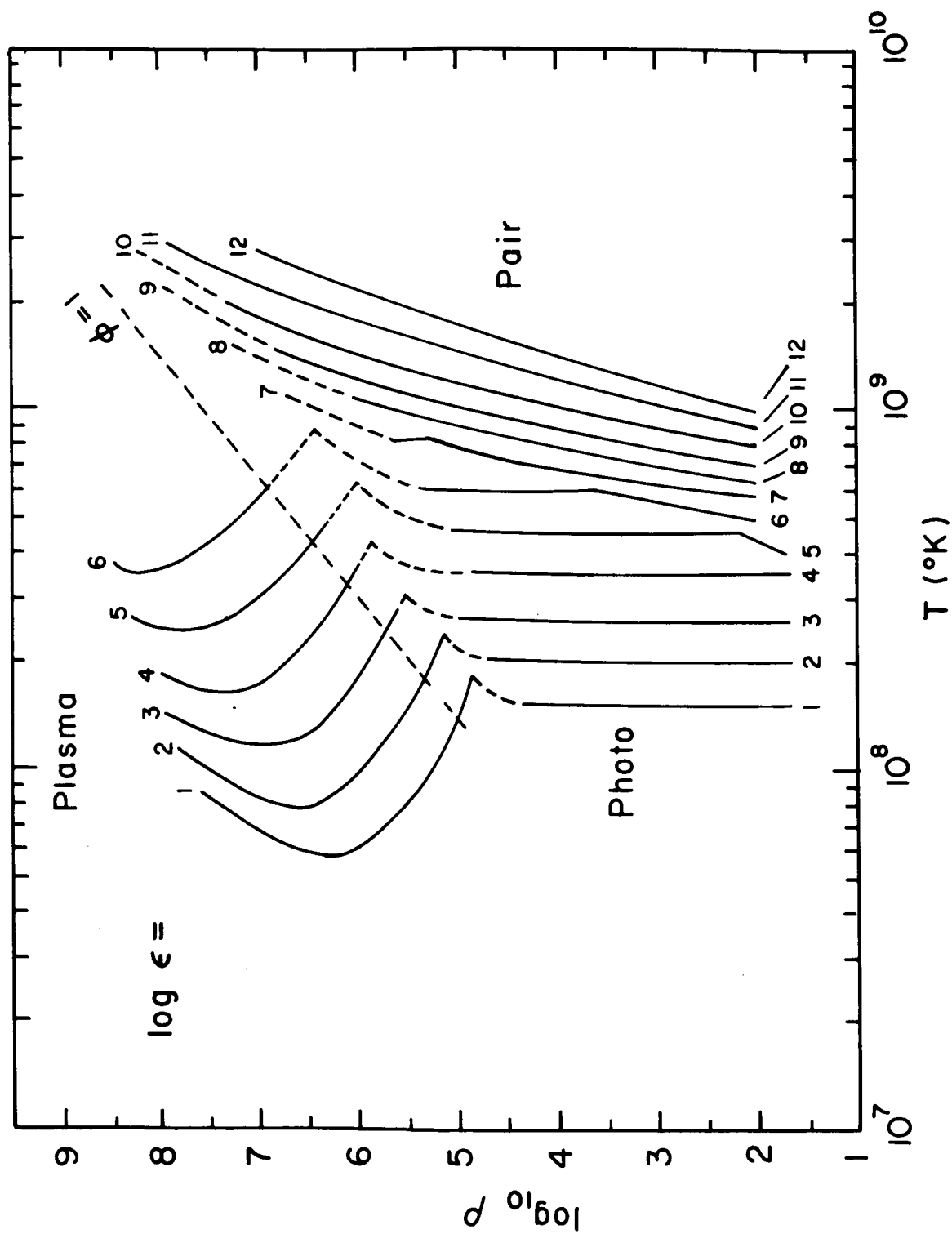
Figure 2.   Densities and temperatures in hydrogen-burning core
   and shells for stars of 1.09, 4 and 15.6 solar masses. The
   numbers on the curves identify the length of time elapsed
   since the beginning of the hydrogen-burning phase and,
   further out on the curves the length of time since the
   onset of the hydrogen burning shell. The results are from
   Hayashi et al (1962).

Figure 2.
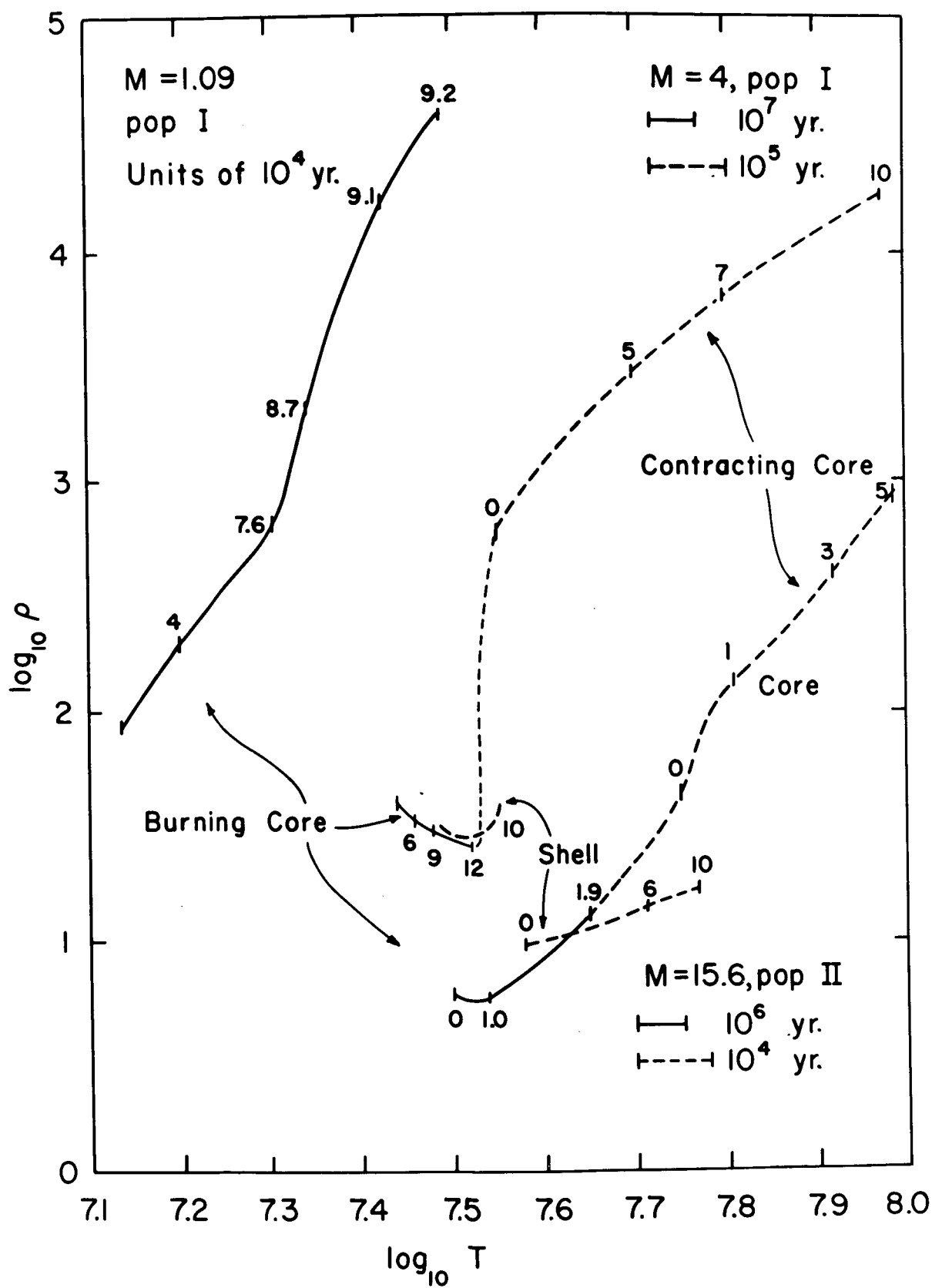
Figure 3. Rates of various nuclear reactions of importance
    during the helium burning phase. The electron screening
    factors are not included here. This effect will be
    important mostly during the period preceding the nitrogen-
    helium flash in small stars.

Figure 3.
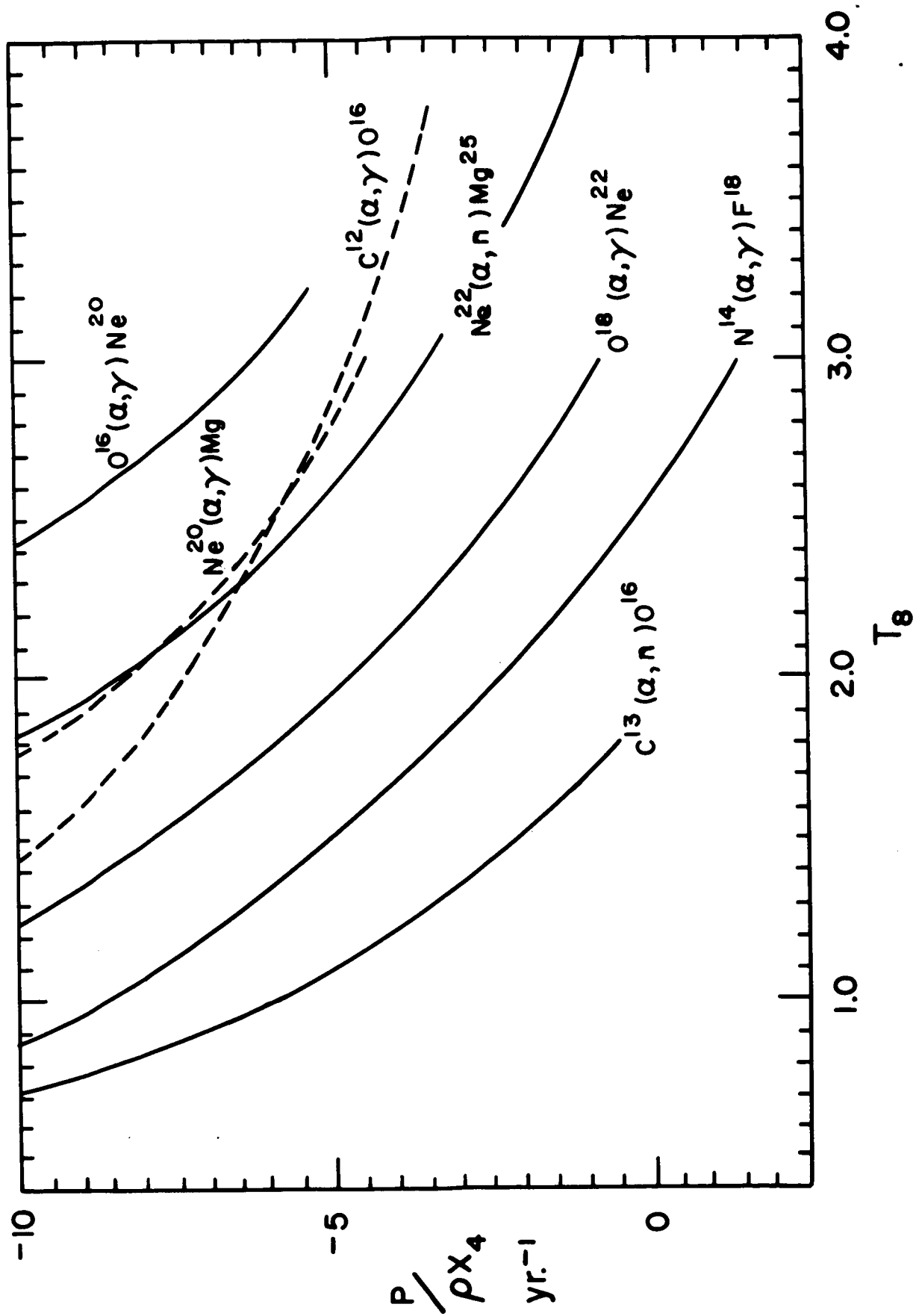
Figure 4. Behaviour of various quantities during the pre-
helium flash period of a $1.2 M_\odot$ star. The calculations
have been made using a sequence of model by Schwarzschild
et al (1962). L/M is the mean energy generation rate for
the whole star (mostly from the hydrogen burning shell).
L_{core}/M_{core} (gravitation) is the energy generation rate from
the contraction of the helium core, $\bar{L}_\nu$(core) is the rate of
neutrino dissipation by plasma neutrino processes. $\bar{\epsilon}_{12}$ core
is the nuclear energy released by the $3He^4 \to C^{12}$ burning.
$\bar{\epsilon}_{13}$, the energy from the $C^{13}(He^4,n)O^{16}$ reaction assuming
$X_{13} = 10^{-4}$ (Pop I star). $\bar{\epsilon}_{14}$ the energy from the $N^{14}(He^4,\gamma)F^{18}$
$(\beta^+,\nu)O^{18}$ assuming $X_{14} = 10^{-2}$ (Pop I star) or $X_{14} = 10^{-3}$
(Pop II star). The effect of these two last nuclear reactions
on the sequence of models have been neglected. (Calculation
by A. Liebman)

Figure 4.
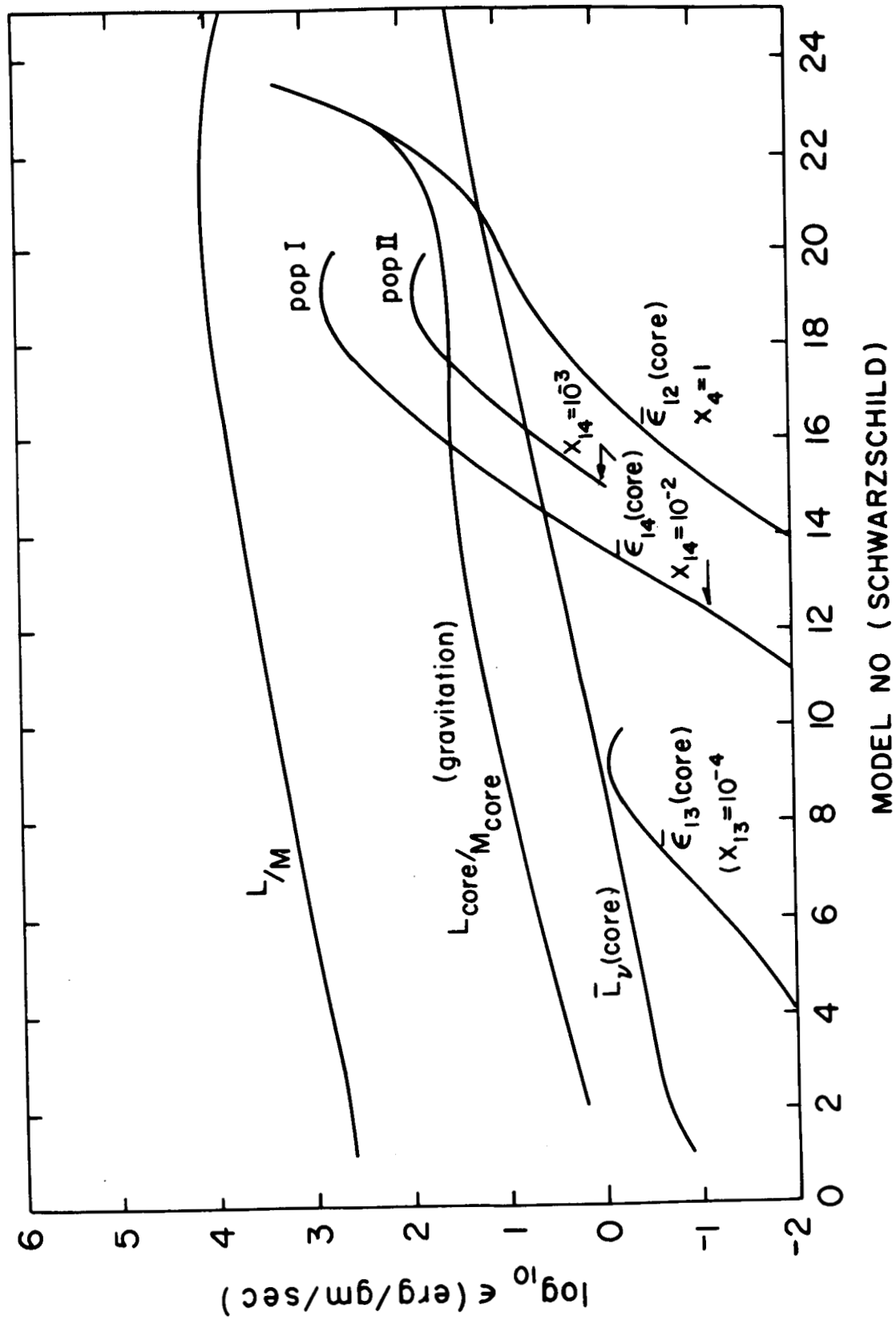
Figure 5. Energy dissipation rate from plasma neutrinos in
erg/gm/sec as a function of T_8 (as a parameter) and
log ρ (as the ascissa).

Figure 5.
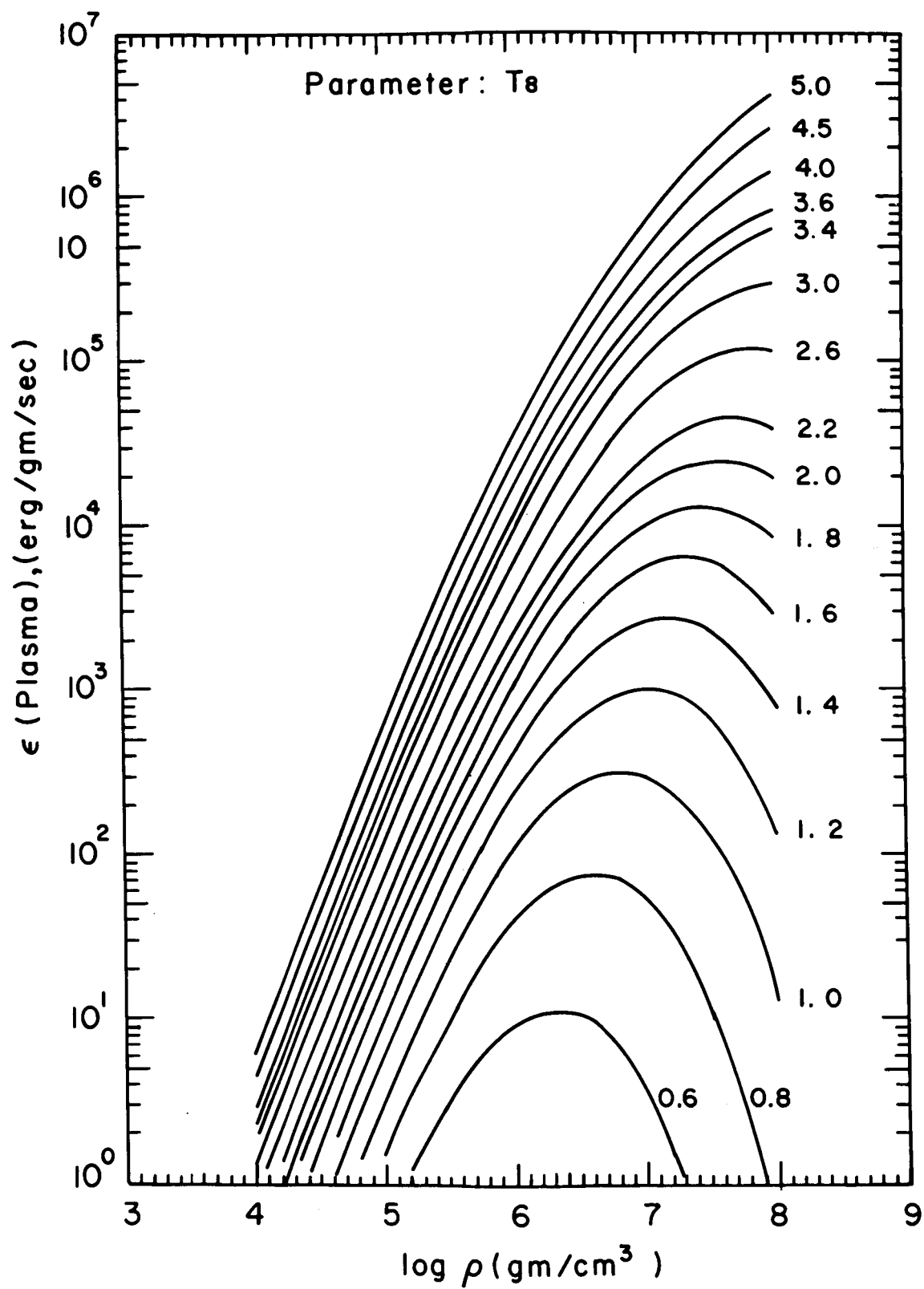
Figure 5.

Figure 6. Densities and temperatures in helium-burning core
and shells and carbon-burning core for stars of 0.7, 4 and
15.6 $M_{\odot}$. The numbers on the curves identify the fractional
weight of helium left in the core. The calculations pertain-
ing to the carbon-burning phase do not take into account the
effect of neutrino dissipation processes. The results are
from the work of Hayashi et al (1962).

Figure 6.
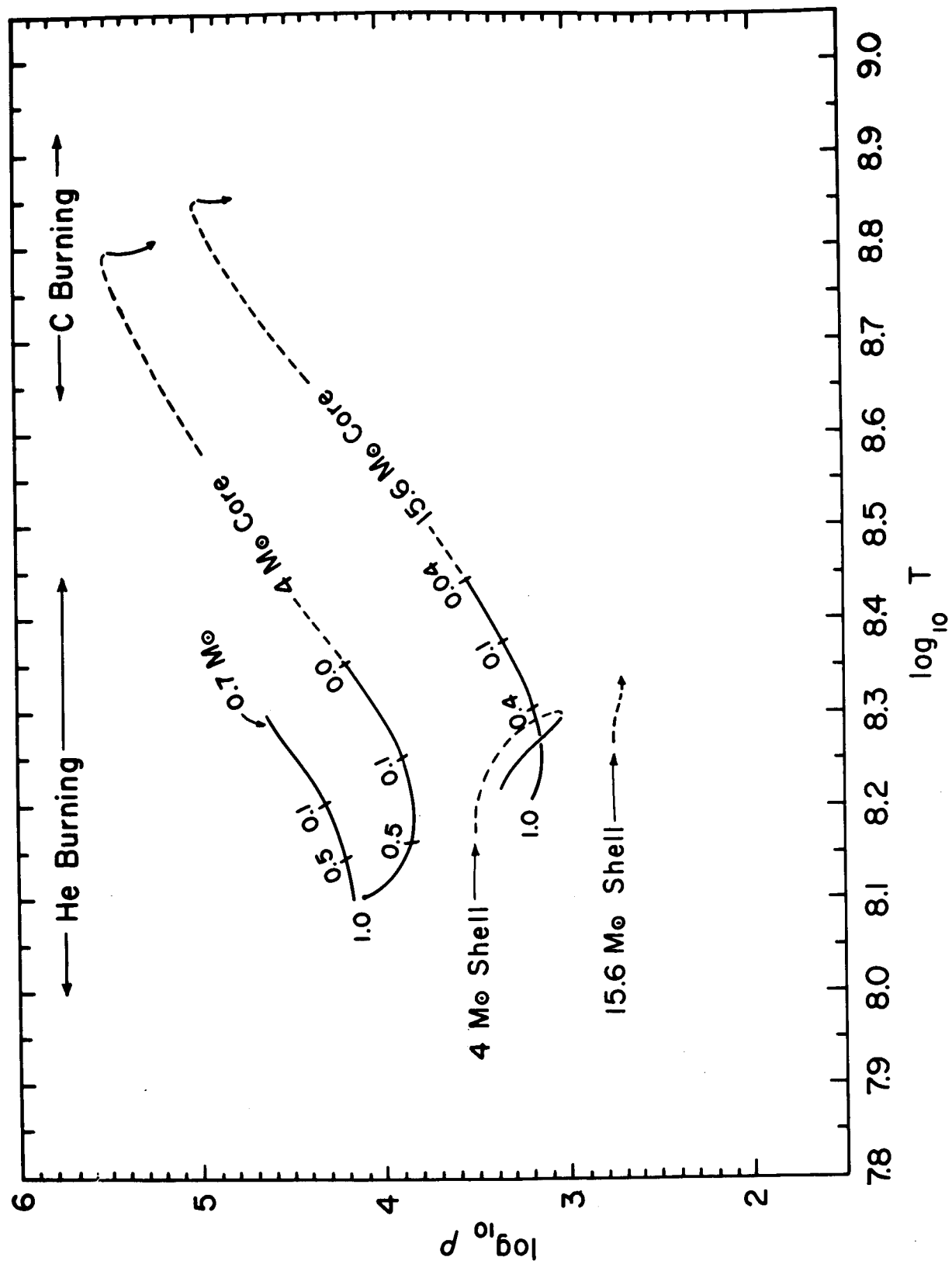
Figure 7. Iso-abundance curves describing isotopic outcome of helium burning processes as a function of (fixed) density and temperature. Except for Neon, only the most important species is mentioned at any point of the ρ-T plane. The caption e,g. C^{12} >50% in a given region means that in the physical conditions pertaining to that region the fractional weight of C^{12} is more than 50% (but less than 80%). The rates used in this figure differed slightly from the rates quoted in the text. Present rates would allow Ne^{20} to go to about 20% in the region where $Ne^{20} \sim 10\%$ is quoted. Everywhere else the abundance of Ne^{20} is at best a few percent.

Figure 7.
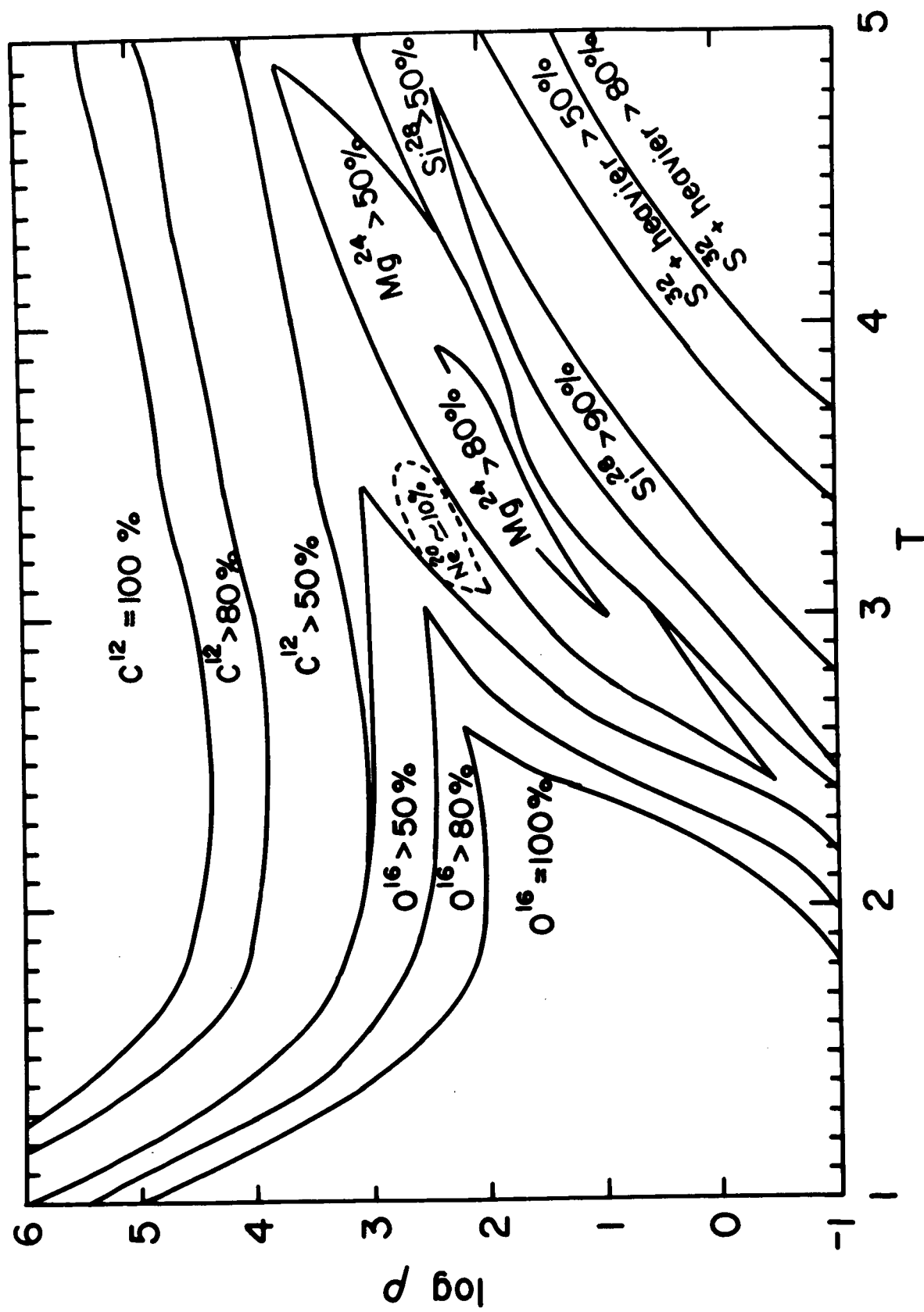
Figure 8. Iso-abundance curves describing the isotopic outcome of the helium burning phase as a function of stellar masses. (Salpeter and Deinzer (1964);pure helium stars). Three curves are given for C^{12} and O^{16}, representing the choice of 0.1, 0.4 and 1.0 for the value of the parameter θ_α^2 (see text). The values of Ne^{20} and Mg^{24} are practically independent of the choice of θ_α^2 .
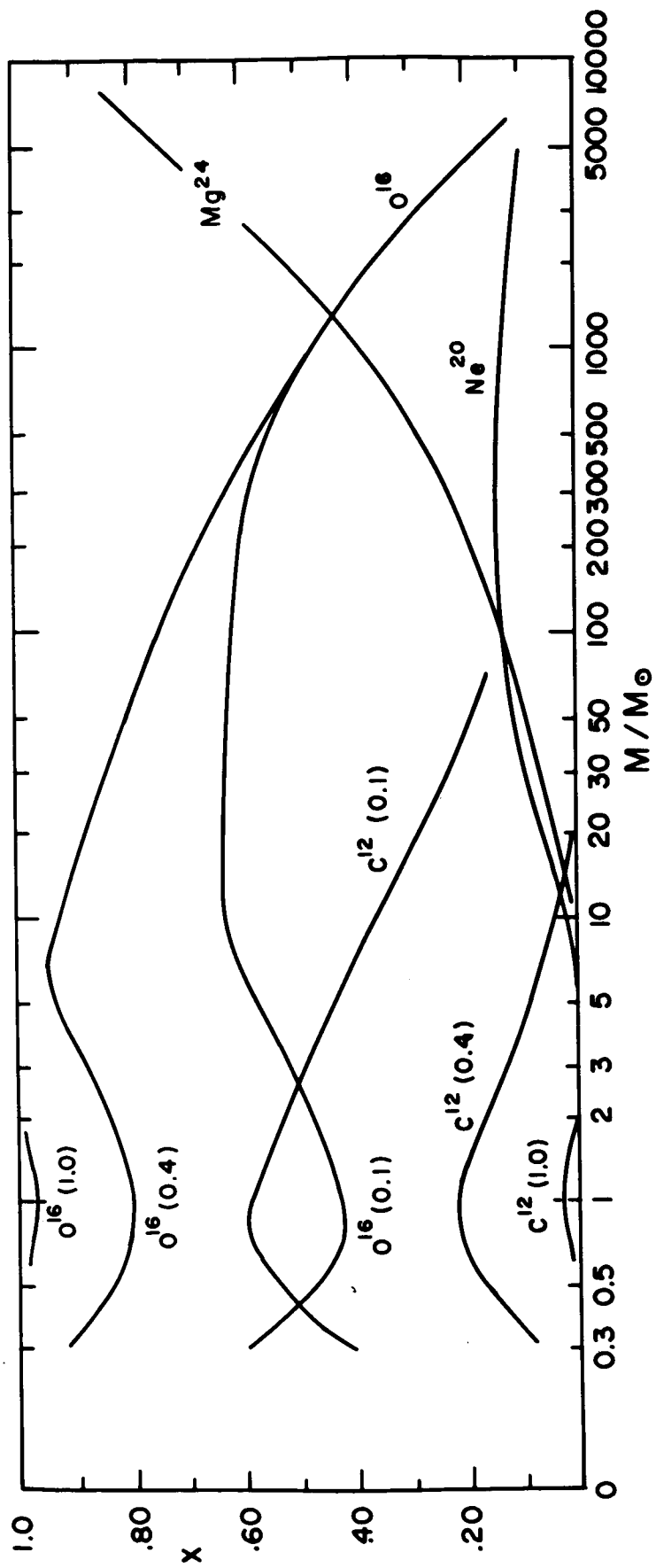
Figure 8.

Figure 9. Energy dissipation by pair annihilation neutrinos in erg/gr/sec. The alscissa is T_8 and the parameter log ρ en gm/cm^3.
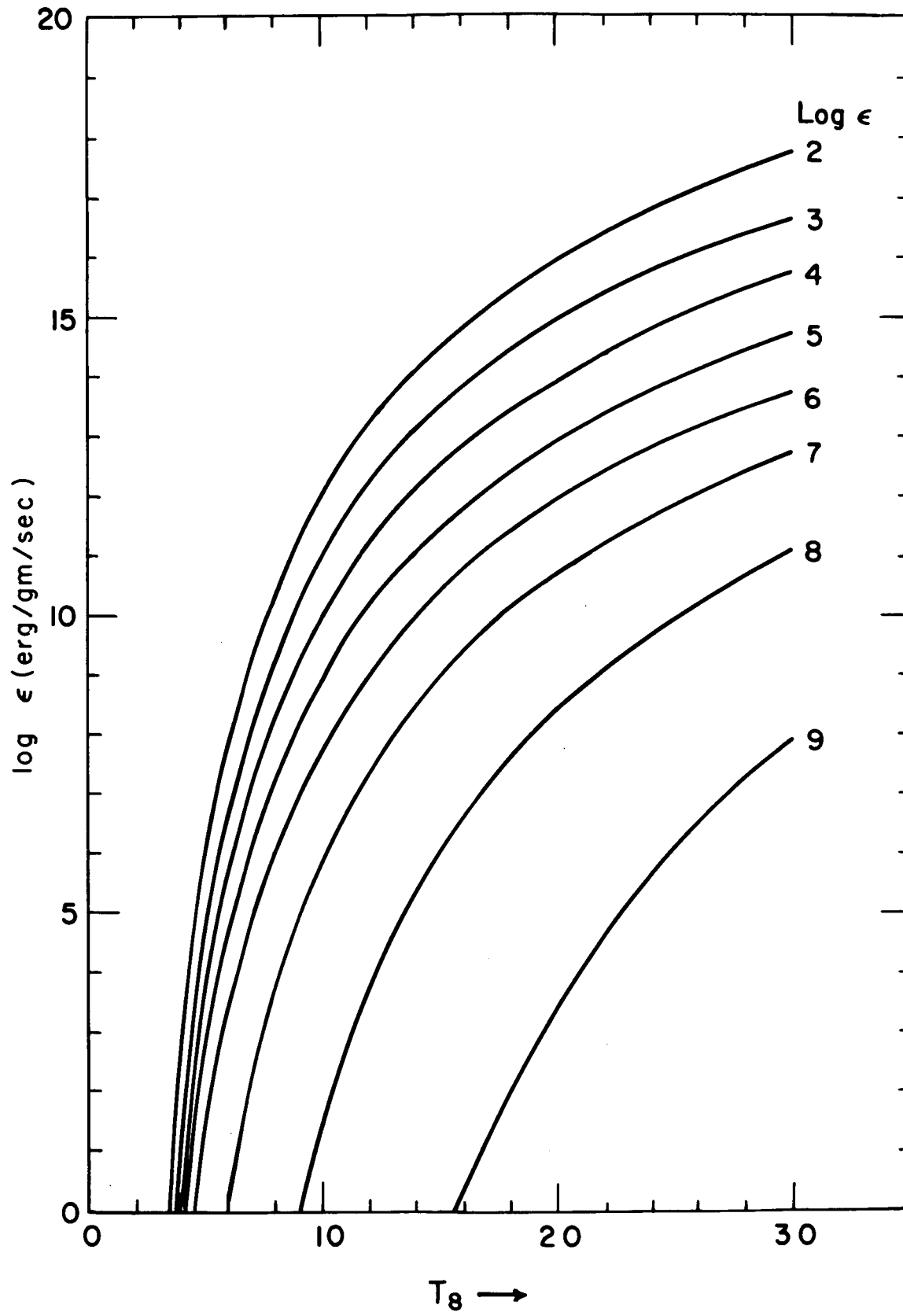
Figure 9.

Figure 10. Carbon-burning stage curves. The "first model"
    line describes the central stellar conditions where the
    nuclear energy generation rate (from $C^{12} + C^{12}$) equals
    the neutrino energy dissipation rate in the center of the
    star. The "corrected model" curve described the central
    stellar conditions when the total (volume integrated)
    nuclear energy generation rate equals the total neutrino
    energy dissipation rate (assuming an $n = 3$ polytropic
    model).

Figure 10.
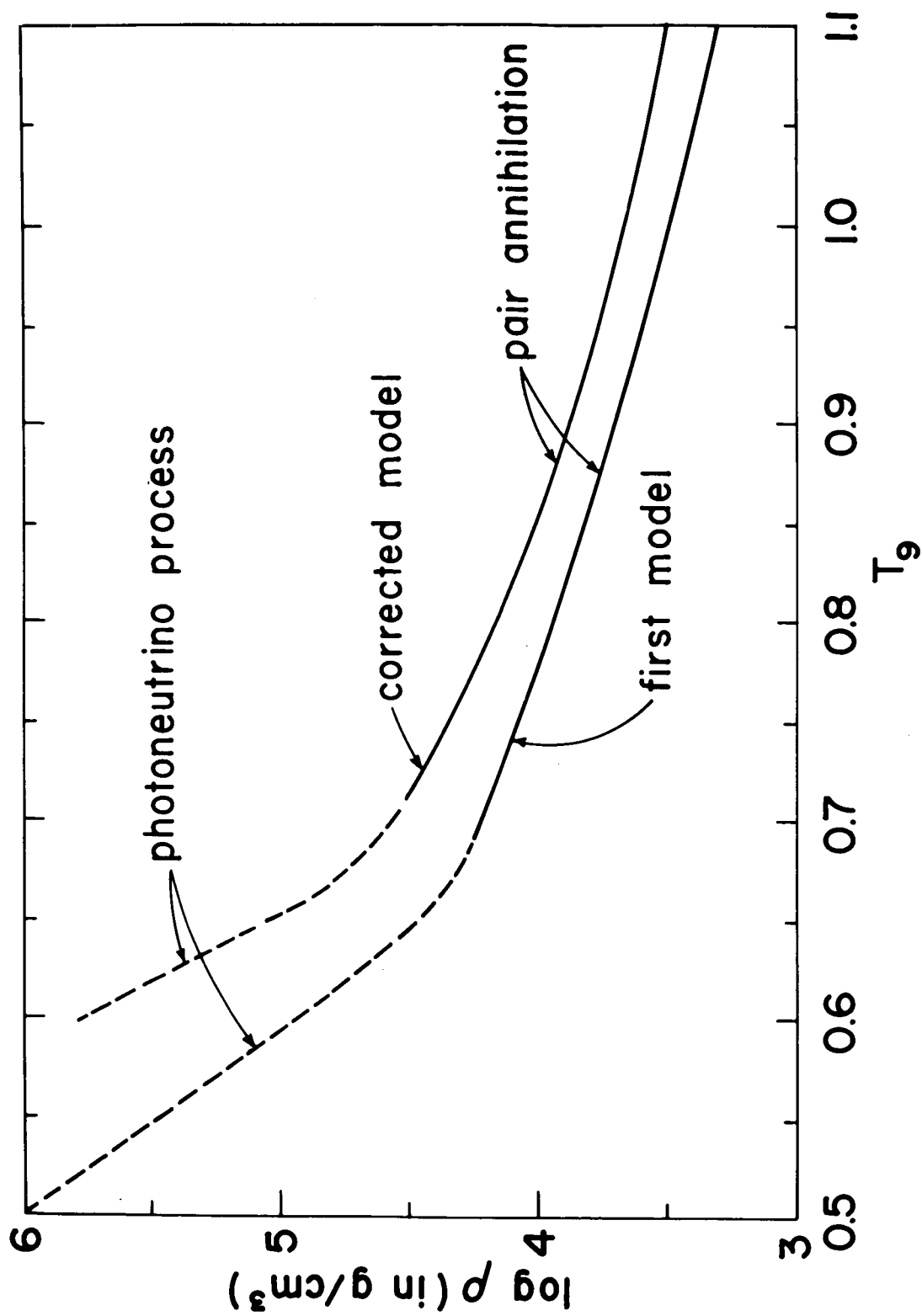
Figure 11. Lifetime and energy generation rate of the carbon
burning stage as a function of the central temperature
using the values given in Figure 10 and described in the
text.

Figure 11.
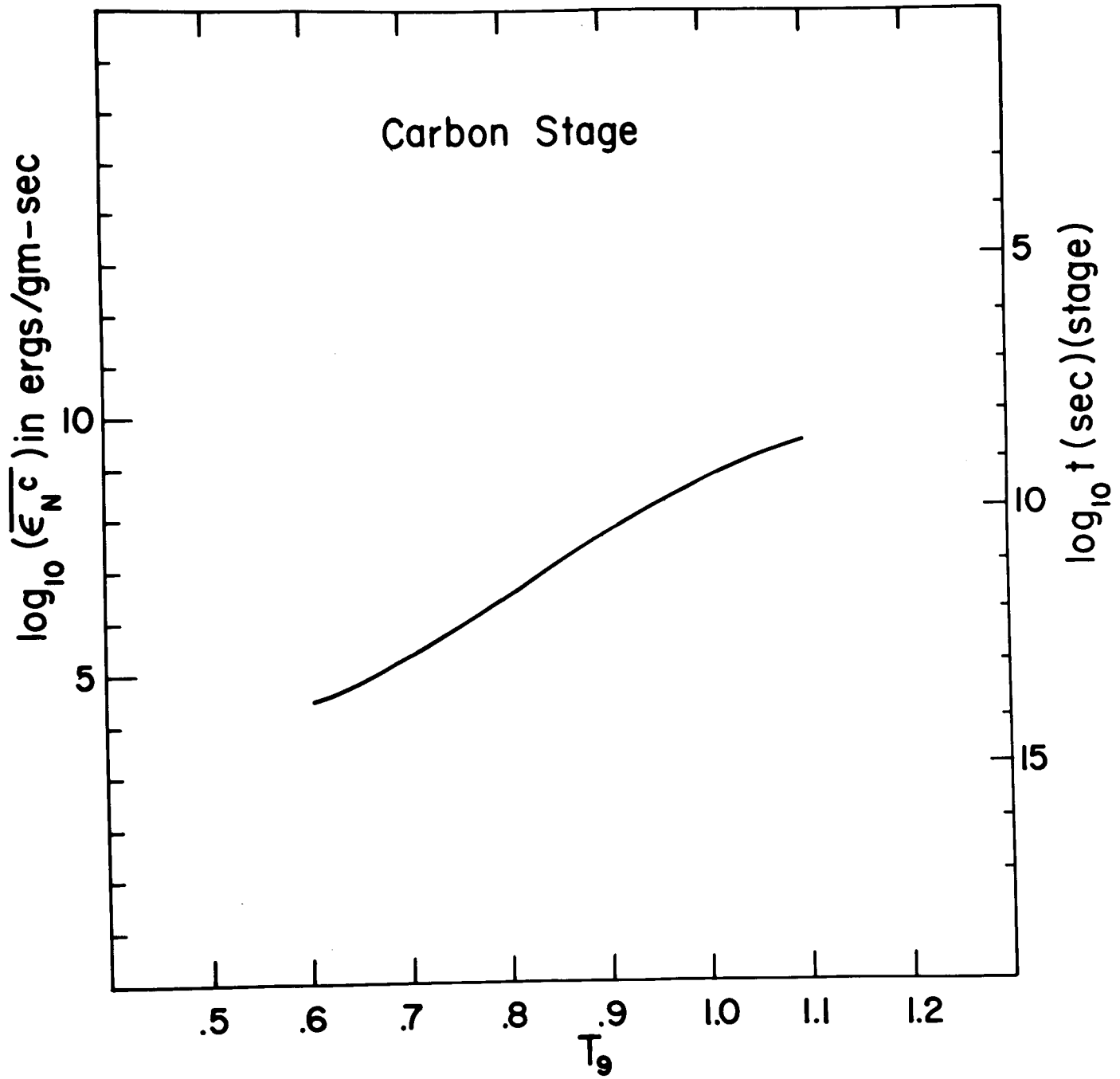
Figure 12. Oxygen and neon-burning stage curves. The model is described in the text and in the caption of Figure 10.

Figure 12.
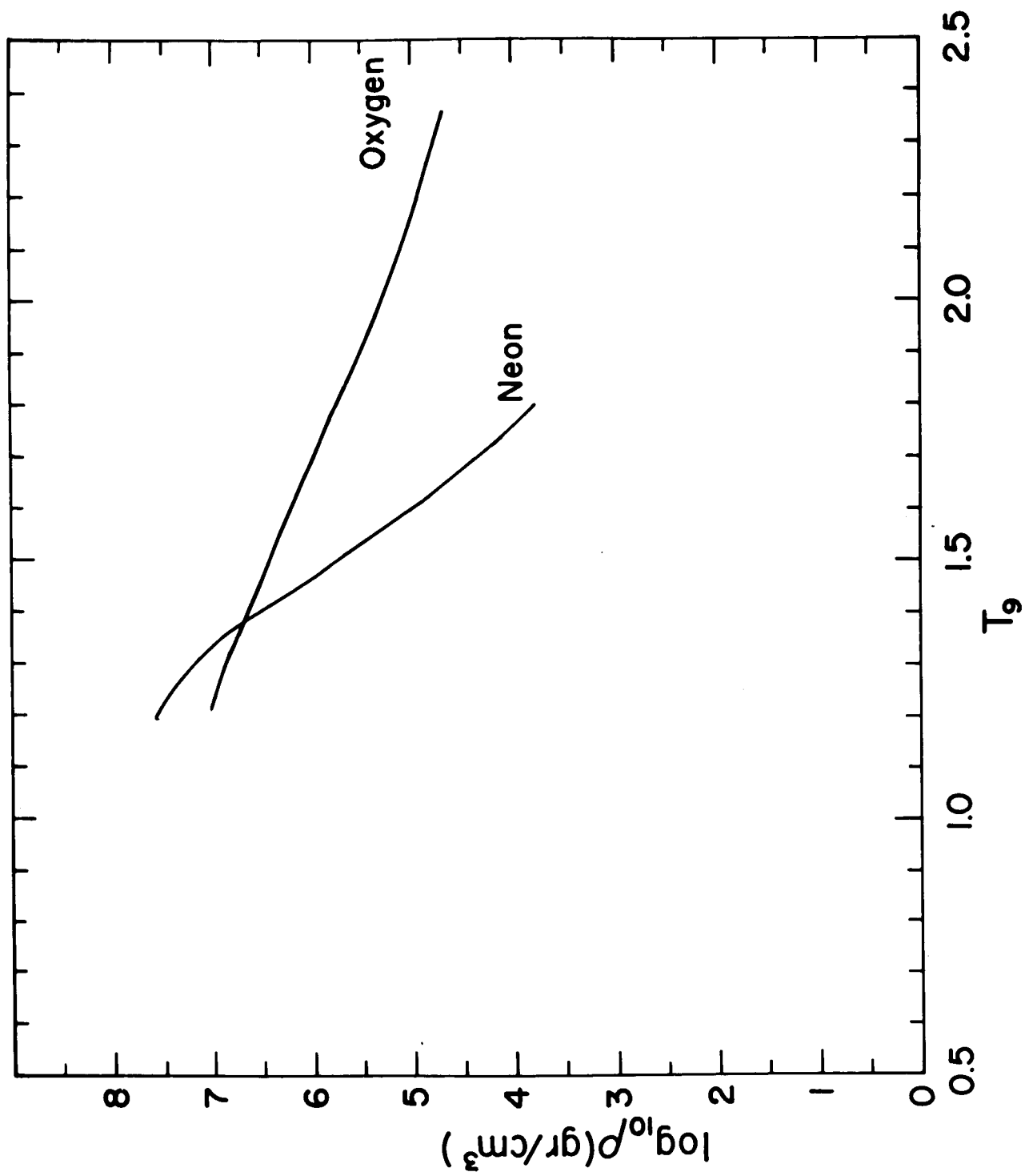
Figure 13. Graph of $\overset{\infty}{\underset{\ell}{\Sigma}} (2\ell+1) g_\ell^{-2}/g_o^{-2}$ as a function of $y^{1/2}$
(see eqn. A3). The graph is valid for $y^{1/2} > 4$, and when
the relative energy is less than one-half of the Coulomb
barrier energy ($B = Z_1 Z_2 e^2/R$).

Figure 13.
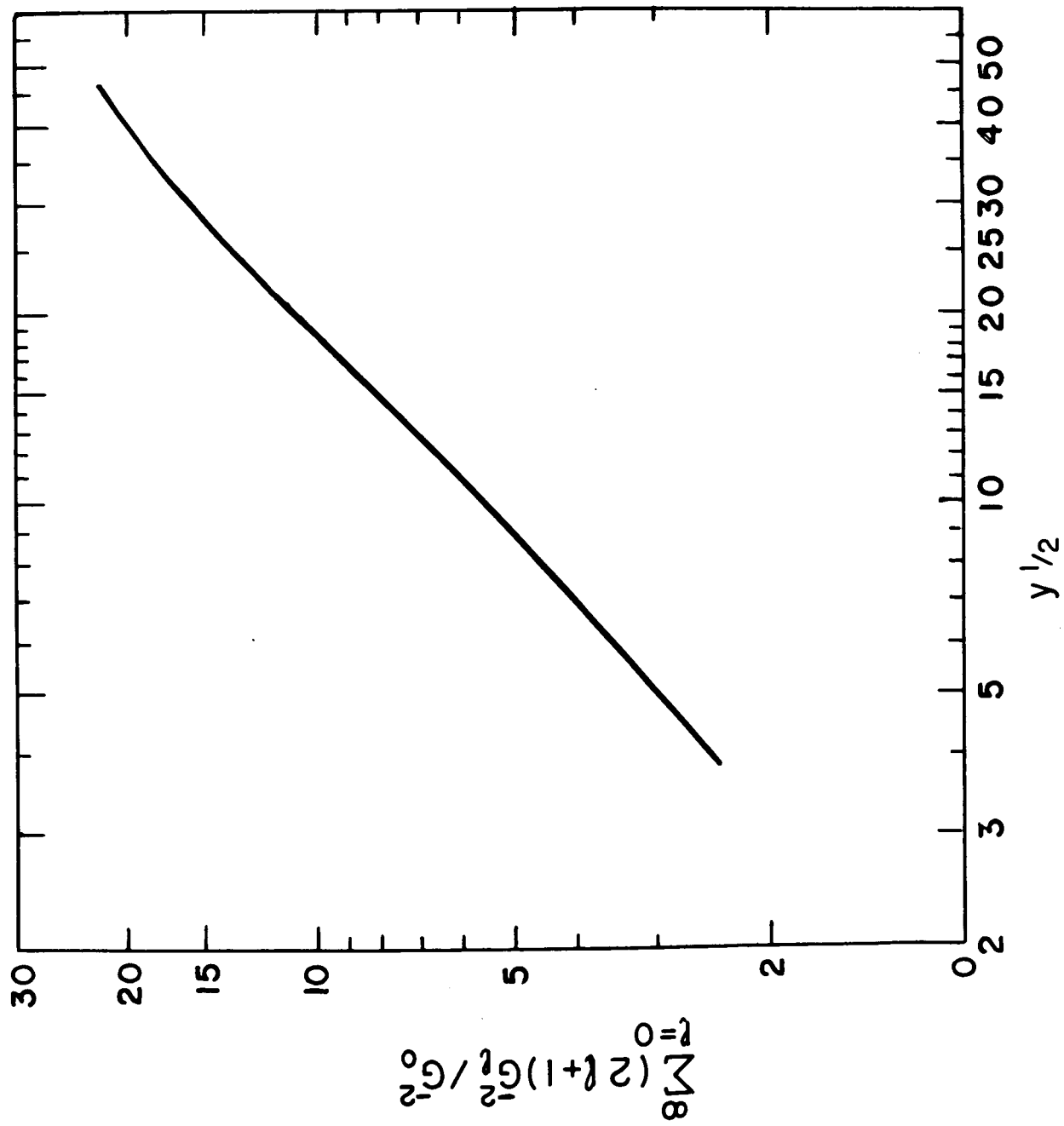
Figure 14. Values of the parameters S and g (see App. A) as a
function of the target nucleus for (α, γ) reactions The
points refer to the results of optical model calculation,
to the matching formula eqns.(A5) and (A7), and for $Ne^{20}(\alpha, \gamma)$
and $Mg^{24}(\alpha, \gamma)$ to a determination of the strength function
from the level scheme of the compound nucleus. (Calculations
by A. Weiswasser)

Figure 14.
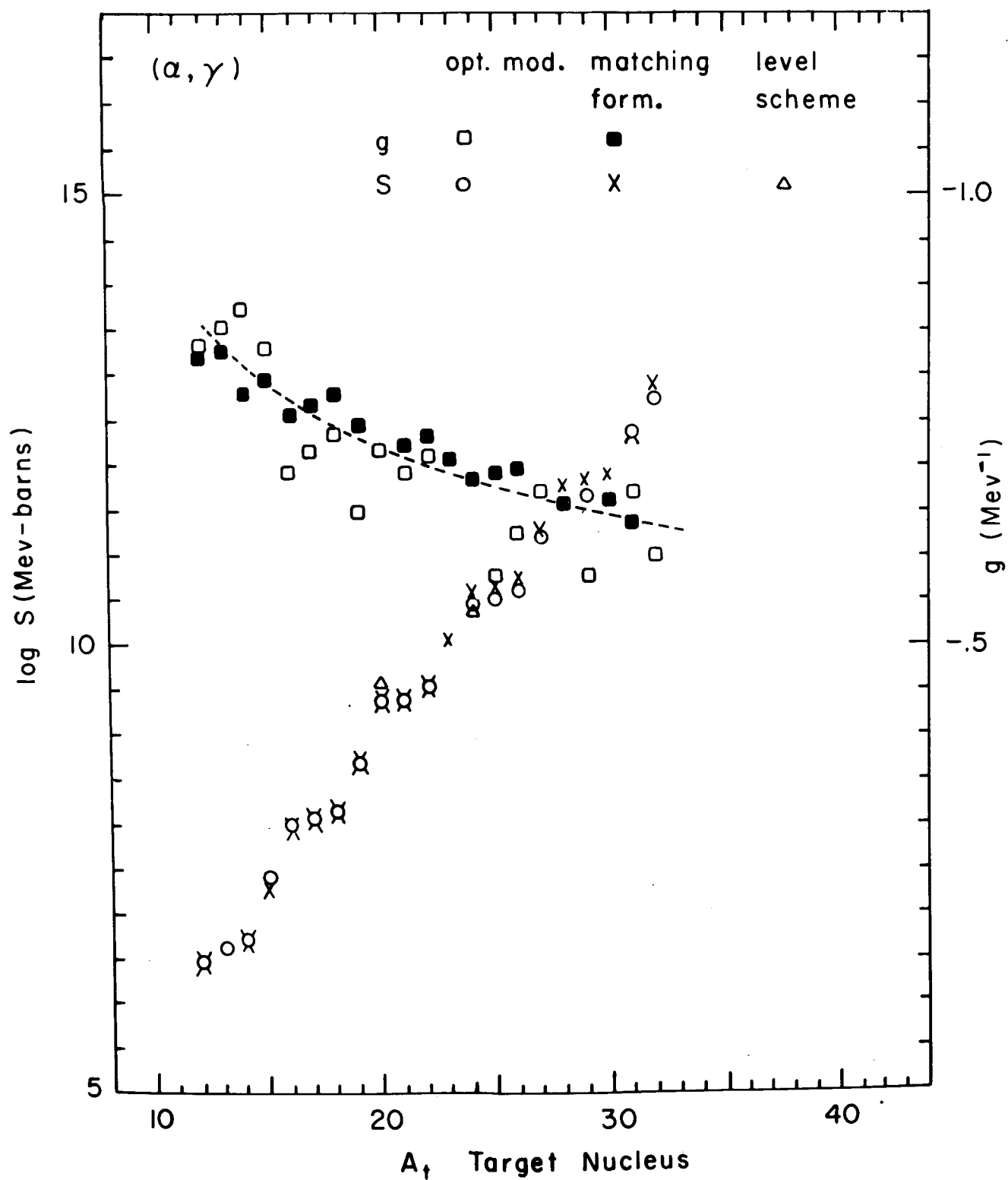
Figure 15. Rate of $Mg^{24}(\alpha,\gamma)Si^{28}$
   The sum over individual resonances (---) is expected to be
   best in the range from $6 < T_8 < 10$. Below and above this
   range unanalyzed resonances are expected to play a role
   hence to increase the rate. The curve called optical model(- ·-)
   is best in the range $T_8 = 3$ to about 10. Below this temperature
   the randomness in the position of the levels makes of it an
   upper limit. Above this temperature the fact that Γ_α becomes
   larger than Γ_γ makes again of it an upper limit, (the optical
   model yields only the total capture rate). The intermediate
   curve in the higher temperature range is based on the experi-
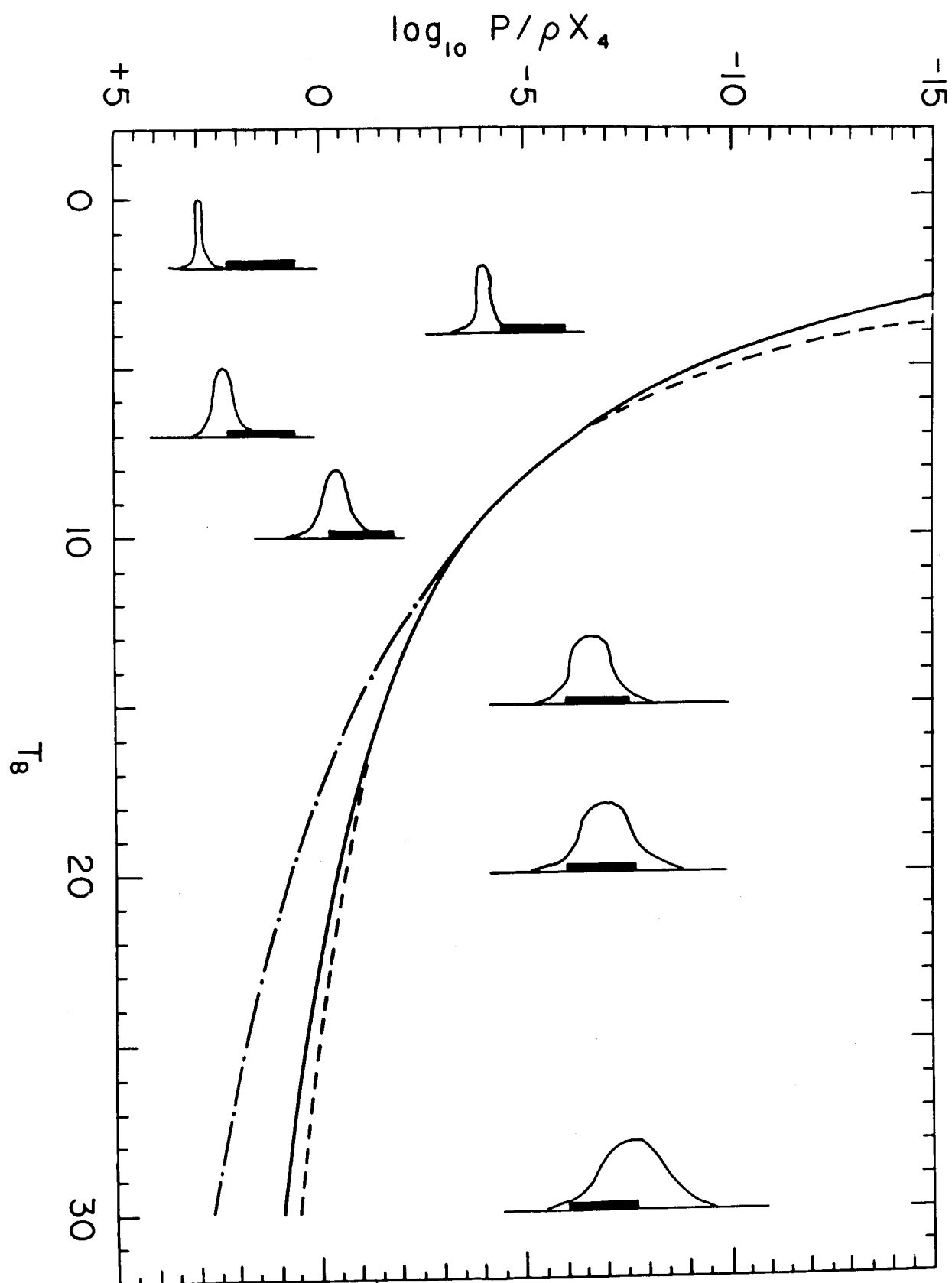   mental gamma strength function. It should be best there.

Figure 15.

Figure 16. The $C^{12} + C^{12}$ total reaction rate.
The (·—·—) curve represents the experimental results.
The solid curve is the result of the optical model. The
dashed curve (merging in the solid curve at low energy) is
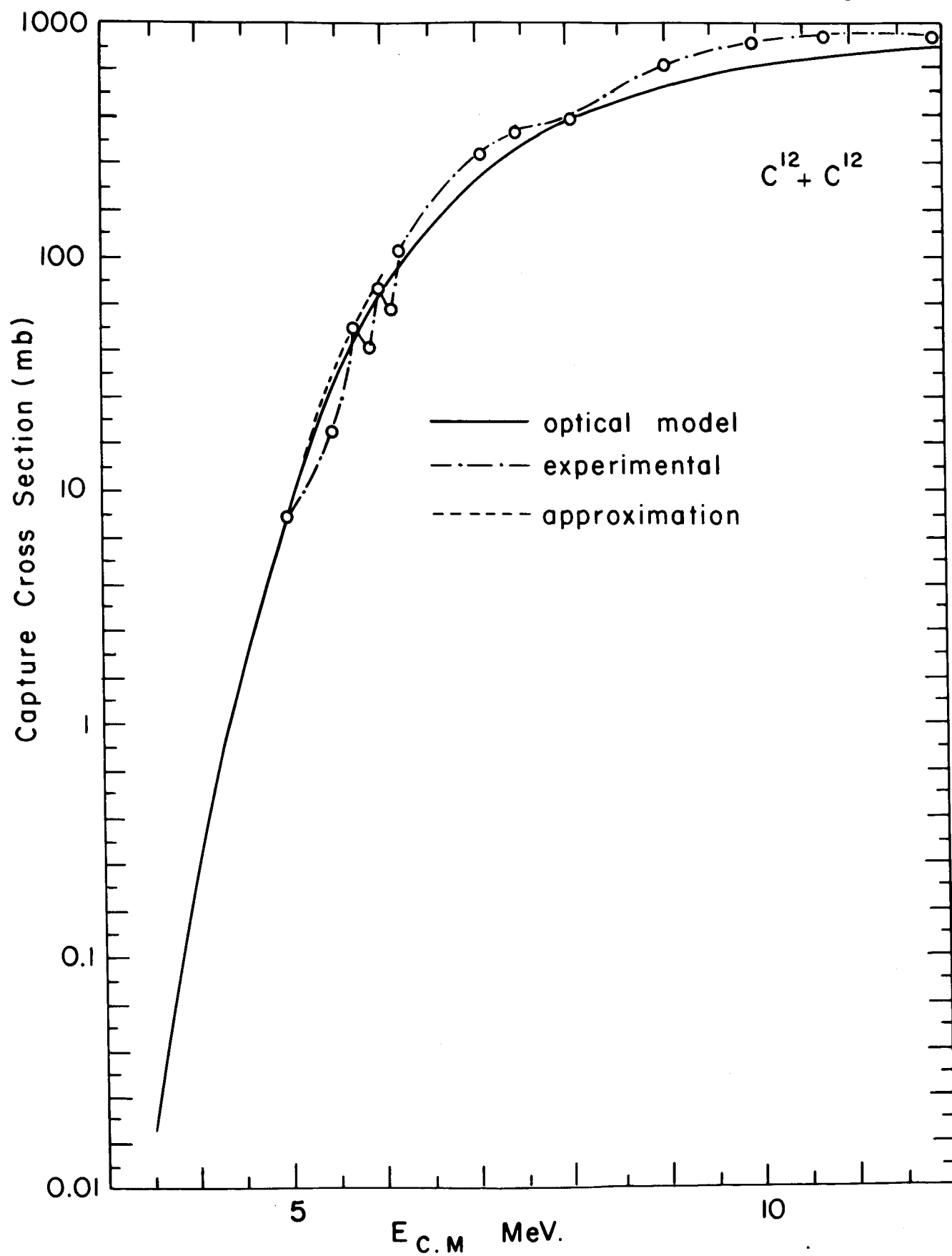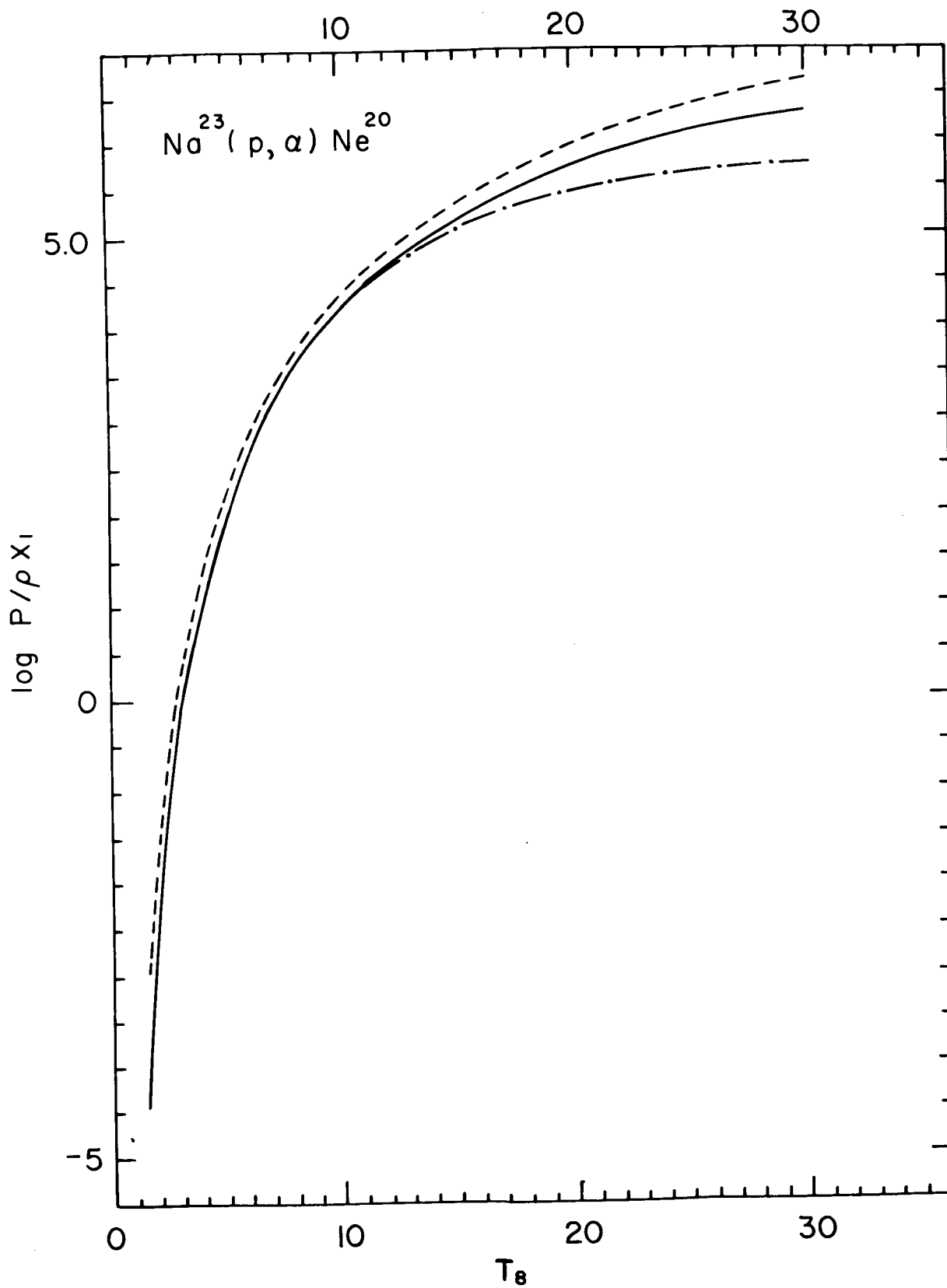obtained from the fitting equation no   .

Figure 16.

Figure 17. Rate of the $Na^{23}(p,\alpha)Ne^{20}$
The dashed line (---) is the sum of individual rates.
It should be correct in the range $T_8 < 10$. Missed
resonances make of it a lower limit at higher temperature.
The dotted line (.—.) has been obtained with the equi-
valent of a strength function. It overestimates the rate
at $T_8 > 15$. There a best choice rate is quoted (——).
(Calculation by Jay Hauben)

Figure 17.

$Na^{23}(p,\alpha)Ne^{20}$

$\log P/\rho X_1$

T_8

ACKNOWLEDGMENT